**The University of Sydney**

Department of Civil Engineering
Sydney NSW 2006
AUSTRALIA

http://www.civil.usyd.edu.au/

**Environmental Fluids/Wind Group**

# A New Design Method for Wave-Induced Pipeline Stability on a Sandy Seabed

**Research Report No R860**

**Fuping Gao, BE ME PhD**
**Dong-Sheng Jeng, BE ME PhD**

**December 2005**

ISSN 1833-2781

The University of Sydney

**Department of Civil Engineering**
**Environmental Fluids/Wind Group**
**http://www.civil.usyd.edu.au/**

# A New Design Method for Wave-Induced Pipeline Stability on a Sandy Seabed

**Research Report No R860**

**Fuping Gao, BE ME PhD**
**Dong-Sheng Jeng, BE ME PhD**

**December 2005**

## Abstract:

The existing DnV Recommended Practice (RP E305) for pipeline on-bottom stability is mainly based on the Pipe-Soil Interaction Model proposed by Wagner et al. (1987) and the Wake Model by Lambrakos et al. (1987) to calculate the soil resistance and the hydrodynamic forces upon pipeline, respectively. Unlike the methods in the DnV Practice, in this paper, an improved analysis method is proposed for the on-bottom stability of a submarine pipeline, which is based on the relationships between and for various restraint conditions obtained by the hydrodynamic loading experiments, taking into account the coupling effects between wave, pipeline and sandy seabed. The analysis procedure is illustrated with a detailed flow chart. A comparison is made between the submerged weights of pipeline predicted with the DnV Practice and those with the new method. The proposed analysis method may provide a helpful tool for the engineering practice of pipeline on-bottom stability design.

## Keywords:

Submarine pipeline; Analysis method; On-bottom stability; Sandy seabed; Wave-pipe-soil coupling effect.

## Copyright Notice

**Department of Civil Engineering, Research Report R859**
**A New Design Method for Wave-Induced Pipeline Stability on a Sandy Seabed**

d.jeng@civil.usyd.edu.au

ISSN 1833-2781



Published by:
Department of Civil Engineering
The University of Sydney
Sydney NSW 2006
AUSTRALIA

December 2005

This report and other Research Reports published by The Department of Civil Engineering are available on the Internet:

http://www.civil.usyd.edu.au

# Contents

# 1. Introduction

Submarine pipelines are a convenient means to transport natural oil or gas from offshore oil wells to an onshore location. One of the main problems encountered with the use of the pipeline is the wave-induced instability (Herbich, 1985). Under the wave loading, there exists a balance between wave forces, submerged weight of pipelines and soil resistance. To avoid swept sideways, the pipeline ought to be given a heavy enough concrete coating, or it has to be anchored or trenched. However, both designs are expensive and complicated. Thus, a better understanding of the wave-induced pipeline stability is important for pipeline design.

In the past decades, with the increasing demand for submarine pipelines to transport natural oil and gas, many researchers had focused particularly on solving wave-induced pipeline instability problems (Wagner et al., 1987; Brennodden et al., 1989; Allen et al., 1989; Foda et al., 1990). However, this problem has not been fully understood because of the complicated soil behavior and geometry of pipelines (Lawlor and Flynn, 1991). Numerous experimental studies on the lateral stability of un-trenched pipelines have been carried out with cyclic actuator loading methods since the 1980's (Wagner et al., 1987; Brennodden et al., 1989; Allen et al., 1989). Among these, Wagner et al. (1987) improved the Coulomb friction theory into an empirical pipe-soil interaction model, in which the total lateral resistance was assumed to be the sum of the Coulomb friction component and the soil passive resistance component. Brennoden et al. (1989) further proposed an energy-based pipe-soil interaction model, in which the soil passive resistance component is related to the work done by pipe during its movement. It has been reported that remarkable cost benefits can be achieved by reduction of designed weight of pipe, when considering the soil passive resistance (Allen et al., 1989). The aforementioned studies indicated that the traditional design method based on the Coulomb friction theory was too conservative. However, in the above experimental investigations, the wave loads were not modeled with hydrodynamic methods but exerted with mechanical actuators, and no water was filled in the tank. Therefore, the wave-induced sand scour around the pipeline could not be modeled properly. The wave-induced oscillatory flow around the pipeline does not only affect the pipeline but also the seabed. In general, the on-bottom stability of the submarine pipeline is the problem of interaction between wave, soil and pipe, rather than only the pipe-soil interaction under cyclic loading as considered in the previous works.

Numerous hydrodynamic experiments have been conducted to investigate scour under fixed pipelines in the past (Foda et al., 1990; Stansby and Starr, 1992). For example, Stansby and Starr (1992) studied the wave-induced settlement of pipeline. Nevertheless, the horizontal movements were not allowed in their experiments. Thus, the phenomena of on-bottom stability could not be really reflected. On the other hand, Foda et al. (1990) examined the vertical stability of half-buried pipe with wave flume, which no scour was observed in their experiments. Since the flow characteristics around half-buried pipeline is different from that around un-trenched pipeline. In fact, from the aspect of wave-pipe-soil interaction, the breakout of un-trenched pipeline is more complicated than that of half-buried one. To date, no experimental data regarding the lateral stability of un-trenched pipeline is yet available.

This study consists of two components. First, a series of physical modeling for the wave-induced pipeline instability is conducted. The onset of pipe breakout is examined. A simple numerical model is employed to provide parametric study. Second, a new design method for wave-induced pipeline stability is proposed, which will provide costal engineers a guideline.

# 2. Physical Modeling for Wave-Induced Pipeline Instability

The interaction between ocean waves, submarine pipeline and seabed has attracted more and more attention over the past few decades. Coulomb friction theory was employed to estimate the friction force between pipeline and soil, under the action of ocean waves before the 1970's. Actually, Coulomb friction theory is far from the realistic wave-induced pipe-soil interaction. Lyons (1973) experimentally explored the wave-induced stability of untrenched pipeline, and concluded that the Coulomb friction theory was not suitable to describe the wave-induced interaction between pipeline and soil, especially when adhesive clay is involved. This is because that the lateral friction between pipeline and soil should be the function of properties of soil, pipe and wave.

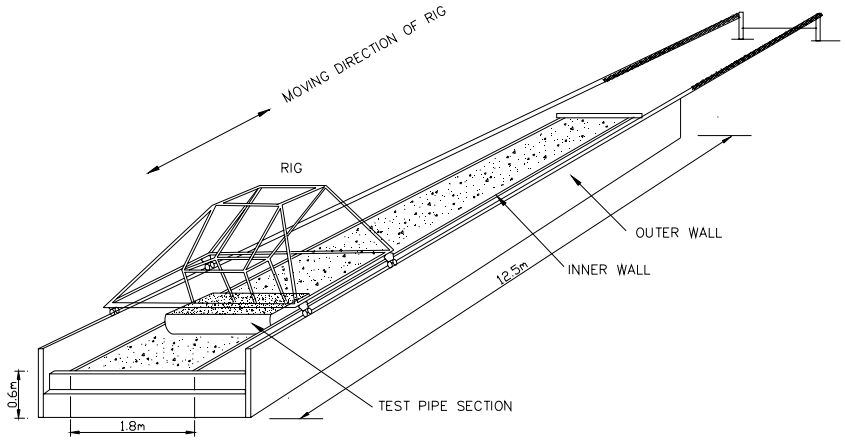


Figure 1: Typical test facility for pipe-soil interaction study by SINTEF (adapted from Wagner et al (1987)0.

Two large model test programs have been conducted by SINTEF in the 1980's, in which the pipeline-seabed interaction was examined with full diameter pipe segments, see Figure 1. These are the multi-client project "PIPESTAB" (1985-87) and the "AGA-project"(1987-88)

(Allen, 1989; Brennodden et al., 1986; Wagner et al., 1987; Brennodden et al., 1989). A considerable experience was gained, including an empirical Pipe-Soil Interaction Model and an Energy Based Pipe-Soil Interaction Model proposed respectively by Wagner et al (1989) and Brennoden et al. (1989), respectively. In both models, the total lateral resistance $F_H$, was assumed as the sum of sliding resistance component $F_F$ and soil passive resistance component $F_R$, i.e.

$$F_H = F_F + F_R \tag{1}$$

where

$$F_F = \mu(W_s - F_L) \tag{2}$$

in which, $\mu$ is the sliding resistance coefficient, $W_s$ is the pipeline submerged weight per meter, $F_L$ is the wave-induced lift force upon pipeline. The difference between two models is the methods for calculating the soil resistance component. In the former model (the Empirical Pipe-Soil Interaction Model, Wagner et al., 1989),

$$F_R = \beta\gamma' A_T, \tag{3}$$

in which $\beta$ is an empirical coefficient, $\gamma'$ is the soil buoyant weight, $A_T$ is half of the contact area between pipeline and soil. However, in the latter model (Energy Based Pipe-Soil Interaction, Brennoden et al., 1989), $F_R$ is relative to the work done by pipe during its movement. These experimental results and the models deduced from the results form an important basis for today's regulations regarding pipeline stability design (Det norsk Veritas, 1988).

In the above experiments, the cyclic loadings are exerted with mechanical actuators to simulate the real wave-induced forces upon pipeline, see Figure 1. Moreover, the pressure upon seabed could not be simulated in their experiments. These pressure fluctuations further induce the variations in effective stresses and pore water pressure within non-cohesive marine sediments. They are different from the actual hydrodynamic wave situations. In reality, the hydrodynamic forces act on not only pipeline but also seabed, and the response of seabed to the hydrodynamic forces can directly affect the pipeline stability. Therefore, precisely speaking, the wave induced on-bottom stability of the submarine pipeline involves the interaction of wave, soil and pipe, not only pipe/soil interaction. Additionally, in the above

Pipe-Soil Interaction Models (Wagner et al., 1989; Brennoden et al., 1989), numerous empirical coefficients have no implicit physical meanings and are difficult to be determined in design procedure. To date, it seems that the underlying physical mechanism is not yet well understood, as stated by Hale et al. (1991).

Regarding the interaction between waves, pipes and sandy seabeds, many investigations have been conducted in the study on sand scouring near pipelines (Sumer et al., 1991; Chiew, 1990; Mao, 1988). In the aforementioned experimental approaches, the pipeline were installed at the fixed condition, thus, the pipeline instability were not involved.

## 2.1 Experimental facilities and instruments

Under the wave action, the water particles oscillate elliptically at upper water level with certain frequency. But due to the boundary effect, the particles near the sea bottom mainly oscillate horizontally, which directly affect the pipeline stability. To simulate the oscillating movement of water particles near the seabed, experiments are conducted in the U-shape oscillatory flow water tunnel, as shown in Figure 2.

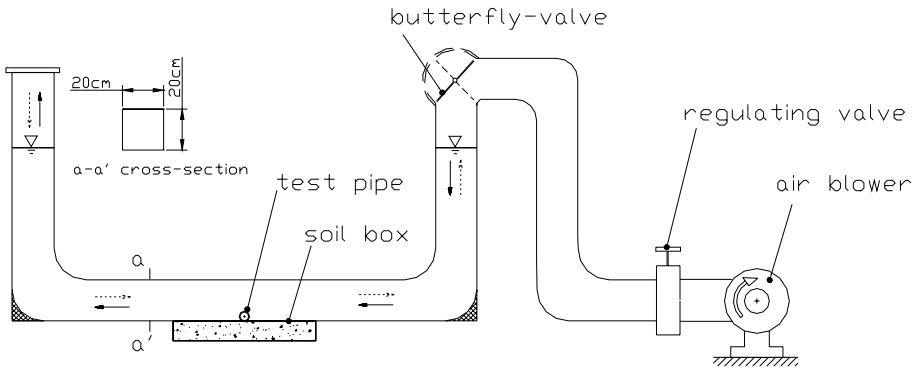


Figure 2: The sketch of U-shaped oscillatory water flow tunnel (Gao et al., 2003)

The water tunnel is made of apparent plexiglass with section area of $0.2\times0.2\mathrm{m}^2$. By a butterfly-valve periodically opening and closing at the top of a limb of the water tunnel, the water accomplishes a simple harmonic oscillation:

$$A = A_0(t)\sin\omega t, \tag{4}$$

in which $A_0(t)$ is the amplitude of oscillatory flow ; $\omega$ is the angle velocity of oscillatory flow, i.e. $\omega = \frac{2\pi}{T}$, $T$ is the period of oscillatory flow, T=2.60(s); $t$ is loading time. By regulating valve, the effective air flux from air blower can be changed. Thus, the amplitude can be varied continuously within 5-200mm.

The lower part of the water tunnel constitutes the test section, under which a soil box with length of 0.60m, width of 0.20m, depth of 0.035m is constructed. The soil box is filled with sand, which is regarded as sand bed at the sea bottom.

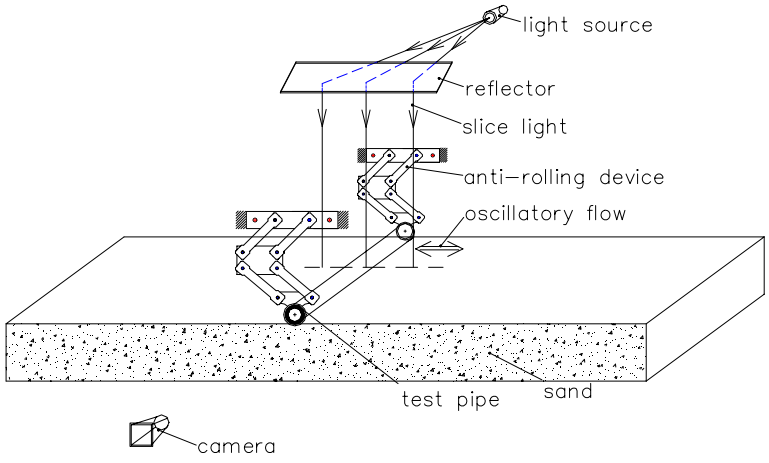


Figure 3: Schematic diagram of testing method.

The test pipe is directly laid upon the surface of sand, as shown in Figure 3. As to a long distance laid pipeline, the stability of pipeline at separate sections is different. For example, the demand for the stability of pipeline sections near risers, is higher than normal sections. In the actual pipeline design, different safety factors are chosen. Due to the constraints from risers and pipeline's anti-torsion rigidity, the movement of the pipeline is not purely horizontal or rotational. Thus, the following two constraint conditions are considered:

**Case I**: pipeline is free at its ends;

**Case II**: pipeline's rolling is restricted, but pipeline can move freely in horizontal and vertical directions. For this purpose, a device for anti-rolling of pipeline was designed (see

Figure3). The anti-rolling device is made of thin plexiglass plate and mini bearings. It includes two parts, which are installed at the two ends of pipeline separately.

To detect the onset of sand scouring, sand scour visualization was carried out under the sliced light by a video camera. Meanwhile, the instability process of the pipe was also observed and recorded by the video camera, as shown in Figure 3.

## 2.2. Froude Modelling

Development and testing of offshore pipeline model is of great importance because of the difficulty of obtaining data from prototypes. However, care must be taken to make sure that the model simulates the behavior of the prototype as accurately as possible.

In the study of wave-pipeline interaction problem, three non-dimensional numbers relative to flow characteristics can be deduced. They are:

(a) Froude number $Fr$

$$Fr = \frac{U_m}{\sqrt{gD}}, \tag{5}$$

which is the ratio of inertia force to gravitational force, which reflects the dynamic similarity of flow with gravity forces acting;

(b) Keulegan-Carpenter number, $KC$

$$KC = \frac{U_m T}{D}, \tag{6}$$

which controls the generation and development of vortex around pipeline, and is related to the hydrodynamic force on the pipe under wave loading;

(c) Reynolds number, $Re$

$$\mathrm{Re} = \frac{U_m D}{\nu}, \tag{7}$$

which is the ratio of inertia force to viscous force.

In the case of ocean wave with a free surface, the gravitational effect predominates, and pipeline on-bottom stability is relative to pipeline's submerged weight. The effect of other factors, such as viscosity, surface tension, etc., is generally small and can be neglected. Since both $Fr$ and Re cannot be satisfied concurrently during model tests, it is convenient to employ the Froude scaling process and allowance is made for variation in Reynolds number (Chakrabrarti, 1994).

According to Froude's law, the following scales should be maintained,

$$\frac{\lambda_{U\,m}}{\lambda_g^{1/2}\lambda_D^{1/2}}=1, \tag{8}$$

where $\lambda$ represents the ratio of the parameters of model to that of prototype.

From (8), since $\lambda_g=1$, we have

$$\lambda_{U\,m}=\lambda_D^{1/2}, \tag{9}$$

$$\lambda_T=\frac{\lambda_D}{\lambda_{U_m}}=\lambda_D^{1/2}. \tag{10}$$

Therefore,

$$\lambda_{KC}=\frac{\lambda_{U_m}\lambda_T}{\lambda_D}=1. \tag{11}$$

This indicates that $Fr$ and $KC$ can be satisfied concurrently during the model tests. Because the Keulegan-Carpenter number follows Froude's law, dependence on KC ensure the model values are applicable to prototype. However, if the quantities strongly depend on Reynolds Number, direct scaling is not possible.

Sandy bottom is distributed in many area in South China Sea, where $Fr$ and $KC$ change between 0-0.5 and 0-20, respectively. In our experiments, the values of $Fr$ and $KC$ vary within these ranges. The Reynolds number is smaller than the actual value by two orders.

## 2.3. Testing materials

### 2.3.1 Soils

Because of the proximity of the pipeline to the seafloor, the modeling of soil characteristic of the foundation may be important. The sand beds consist of medium sand and fine sand. The index properties of the sands are shown in Table 1. The moist sand is first saturated, then packed in the soil box under water, and finally trimmed with a scraper. The difference of the unit weights for different tests is controlled within the error of 5‰.

### 2.3.2 Pipelines

The pipe model spans the soil surface vertically to the direction of oscillatory flow, as shown in Figure 3. The length of the pipe model should be sufficient to minimise the ending effects. To simulate the two dimensional problem, the pipe ends are close to the vertical walls of U shaped tunnel. In the experiments, the gaps between pipe ends and the U shape tunnel walls are about 5 mm. Thus, scouring at the end of the pipe model is not considered a problem, which has been proved in the tests.

The submarine pipeline generally has a large span so that the pipeline model may be treated as a two-dimensional structure. The submerged weight of pipeline directly determines the contact force between pipeline and seabed, and further affects on-bottom stability around the pipeline.

The weight of the pipe is adjusted to model the typical submerged weight of actual pipeline, according to the similarity parameter $G$, i.e.

$$G = \frac{W_s}{\gamma' D^2}, \tag{12}$$

in which, $\gamma'$ is buoyant unit weight of soil, $\gamma' = (\rho_{sat} - \rho_w)g$. That is, the model and prototype can be expressed by

$$G = \frac{(W_s)_p}{\gamma'_p D^2_p} = \frac{(W_s)_m}{\gamma'_m D^2_m}, \tag{13}$$

where the subscripts $p$ and $m$ stand for prototype and model respectively. The testing pipes are composed of aluminium, with length of 0.19m. The pipes are divided into three

groups with different diameters: 0.014, 0.020 and 0.030m. In each group, pipes have different weights. The diameter $D$ and submerged weight $W_s$ of test pipes are listed in Table 2.

Table 2: The parameters of test pipes

| Case I | | | | | | Case II | |
|---|---|---|---|---|---|---|---|
| Pipe diameter $D$ (m) | Submerged weight $W_s$ (N/m) | Pipe diameter $D$ (m) | Submerged weight $W_s$ (N/m) | Pipe diameter $D$ (m) | Submerged weight $W_s$ (N/m) | Pipe diameter $D$ (m) | Submerged weight $W_s$ (N/m) |
| 0.030 | 1.52 | 0.020 | 1.09 | 0.030* | 1.61 | 0.030 | 1.51 |
| 0.030 | 2.00 | 0.020 | 1.35 | 0.030* | 2.00 | 0.030 | 2.04 |
| 0.030 | 2.40 | 0.020 | 1.54 | 0.030* | 2.40 | 0.030 | 2.59 |
| 0.030 | 3.12 | 0.020 | 1.72 | 0.030* | 3.12 | 0.030 | 2.94 |
| 0.030 | 3.53 | 0.020 | 1.97 | 0.030* | 3.53 | 0.020 | 0.78 |
| 0.030 | 3.93 | 0.014 | 0.78 | 0.030* | 3.93 | 0.020 | 0.98 |
| 0.030 | 4.22 | 0.014 | 0.89 | 0.030* | 4.22 | 0.020 | 1.12 |
| 0.030 | 4.40 | 0.014 | 1.05 | 0.030* | 4.50 | 0.020 | 1.29 |
| 0.030 | 5.00 | 0.014 | 1.21 | 0.030* | 5.00 | | |
| 0.030 | 5.24 | | | 0.030* | 5.29 | | |

According to dimensional analysis, (13) can also be expressed as

$$\frac{\lambda_{W_s}}{\lambda_{\gamma'}\lambda_D^2}=1, \tag{14}$$

When $\lambda_{\gamma'}=1$, then the ratio of the pipeline submerged weight of model to that of prototype is

$$\lambda_{W_s}=\lambda_D^2. \tag{15}$$

Due to the pipe weight and the operation reason, some initial embedment always does exist, although the amount of embedment is very small. Conventionally, $e/D$=0.03-0.05, where $e$ is pipe initial embedment.

## 2.4 Testing procedures

To explore the mechanism of pipeline instability induced by rapidly increasing storm wave, a constant velocity of oscillatory flow amplitude $\dot{A}_0$, $\dot{A}_0 \approx 9\times10^{-3}\, cm/s$, was adopted firstly in the experiments.

From equation (4), the velocity of oscillatory flow can be deduced,

$$U(t) = \dot{A}_0(t)\sin\omega t + \omega A_0 \cos\omega t . \tag{16}$$

In the experiments, $A_0(t)$ is the order of $10^{-1}$(m), thus $\frac{\dot{A}_0}{\omega A_0} \approx 0(10^{-3})$. Therefore, the maximum water particle velocity of the oscillating flow $U_m$ is as follows:

$$U_m \approx \omega A_0(t) . \tag{17}$$

In the other words, the maximum water particle velocity is mainly relative to the angle velocity and the current flow amplitude. Furthermore, since the storm growing is not always continuous, it is necessary to examine the effects of loading history on pipeline instability, which will be described in section 2.53.

During the experiments, the water level change was recorded with a water differential pressure transducer and data acquisition system.

## 2.5 Experiment results

### 2.5.1 Pipeline Instability process

When the amplitude of oscillatory flow $A_0$ increase continuously with a constant velocity, the pipeline displacements are recorded (see Figure 4). The following three characteristic times can be identified in the pipeline instability process:

1) $t = t_s$: At a certain distance apart from the pipe, the sand grains at the bed surface start to move visibly. Onset of scour occurs (see Figure 5). When the water particle velocity is large enough to make considerable amount of sediment into suspension, sand ripples are gradually formed in the vicinity of the pipe.

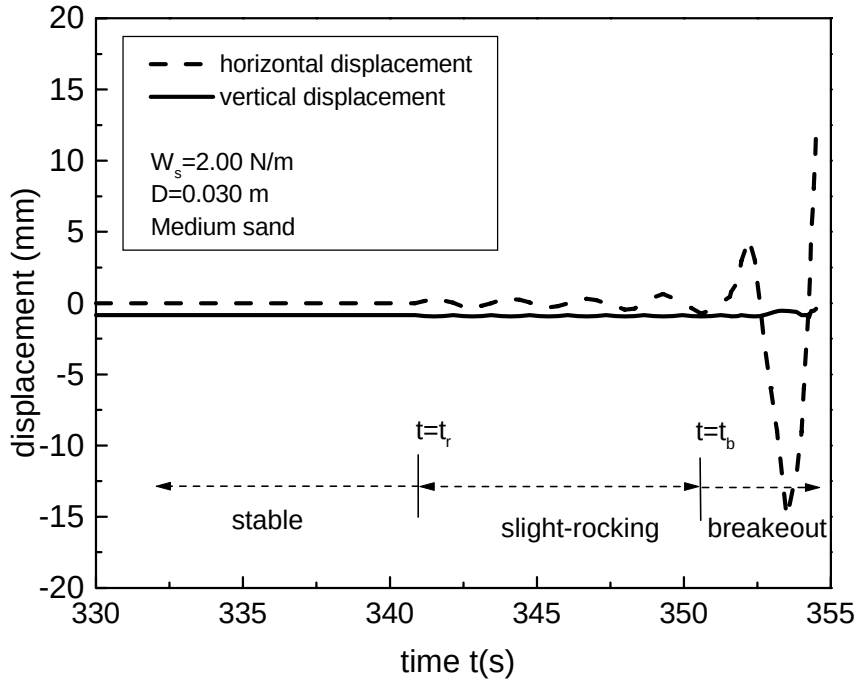


(a) Case I

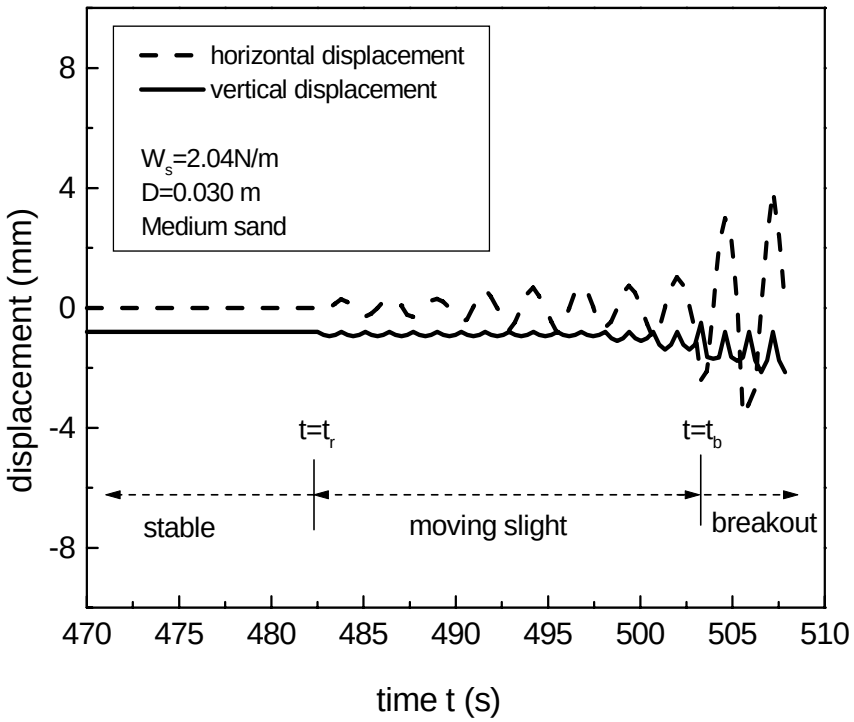


(b) Case II

Figure 4: Pipe displacement-time curves.

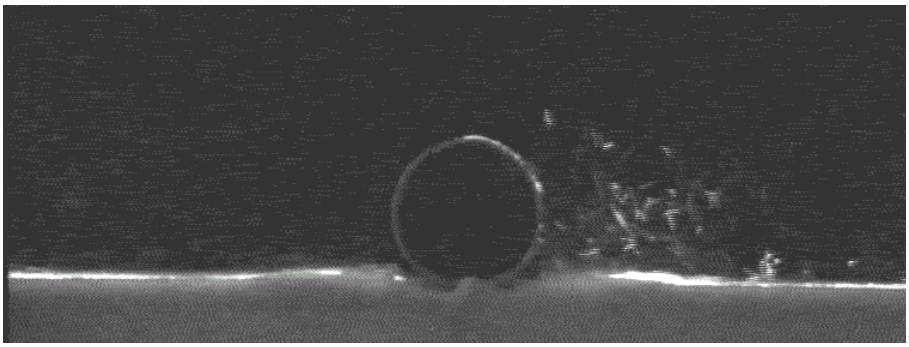

Figure 5: Onset of sand scouring

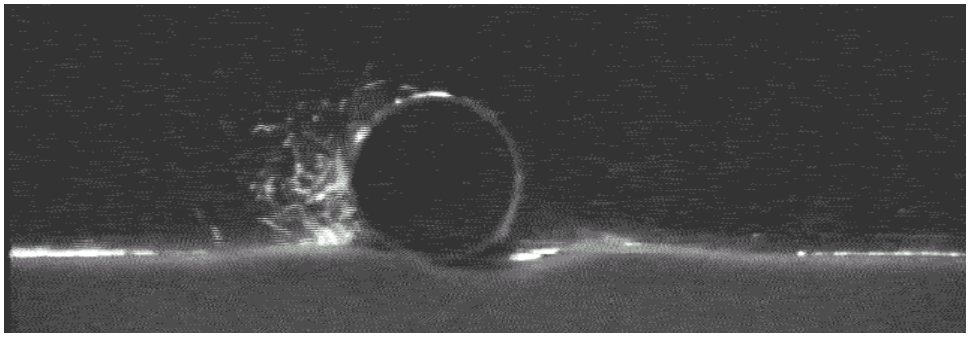

(a) Case I

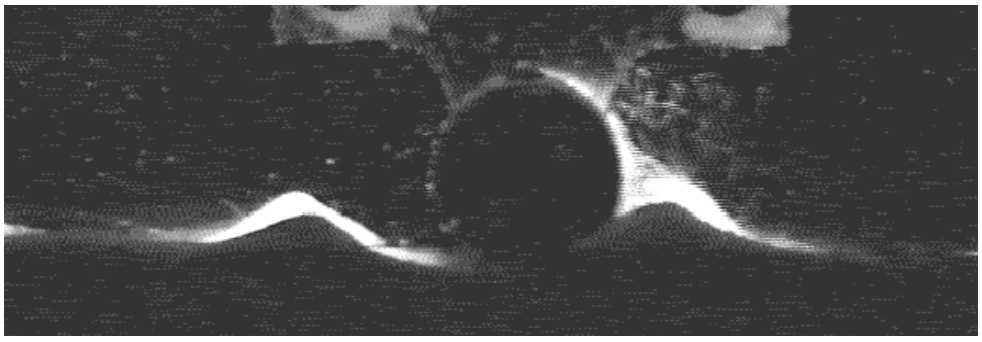

(b) Case II

Figure 6: Phenomena of Pipeline losing stability

2) $t = t_r$: The pipe begins to move slightly (see Figures 4 and 6). As to Case I, pipe mainly swings at its original site, and its vertical settlement is nearly invisible. But for Case II, both vertical and horizontal movements develop gradually. The horizontal displacement is about 1-3%D, while the vertical settlement is approximately less than 1%D.

3) $t = t_b$ : Pipe breakout takes place at a short time (see Figures. 4 and 6). As to Case I, pipe begins detaching from its original place for few cycles. Then it rolls away immediately, and sometimes it rolls over the sand ripple nearby. But, as for Case II, pipe pushes the sand aside with the horizontal displacement of approximate 20-30%D.

The pipeline instability is always coupled with sand scouring. However, as to the pipelines whose submerged weights are small, the pipeline breakouts when the oscillatory flow is not strong enough to induce sand scour.

## 2.5.2. Criterion for pipeline on-bottom instability

The wave-induced instability of pipelines with two constraint conditions, i.e. Case I and Case II, was studied respectively.

**Case I: Freely laid pipeline**

In order to explore the effects of sand properties on pipeline instability, the experiments on the instability of pipelines with various diameters and weights were conducted on medium sand and fine sand separately, whose properties are listed in Table 1. The oscillatory flow amplitudes at which pipe loses stability ( $A_0 = A_b$ ) were recorded. With equation (5), (6) and (17), KC and Fr numbers can be obtained by

$$KC = \frac{2\pi A_b}{D}, \tag{18}$$

$$Fr = \frac{2\pi A_b}{T\sqrt{gD}}. \tag{19}$$

Table 1: Index properties of the test sands

| Mean grain size | Grain size at which 10% of the soil weight is finer | Uniformity coefficient | Unit weight | Dry unit weight | Initial void ratio | Relative density |
|---|---|---|---|---|---|---|
| $d_{50}$ (mm) | $d_{10}$ (mm) | $Cu$ | $\gamma$ $(kN/m^3)$ | $\gamma_d$ $(kN/m^3)$ | $e_0$ | $D_r$ |
| 0.38 | 0.30 | 1.4 | 19.00 | 14.80 | 0.73 | 0.37 |
| **0.21** | **0.11** | **2.0** | **21.05** | **17.47** | **0.56** | **0.60** |

Figure 7 shows the correlation between G and KC number. As to the pipelines with same diameter, KC at which pipelines lose stability increase linearly with G number. But the relationships are different for different diameters. It shows that when using KC number for data reduction, pipeline diameter effect is significant.

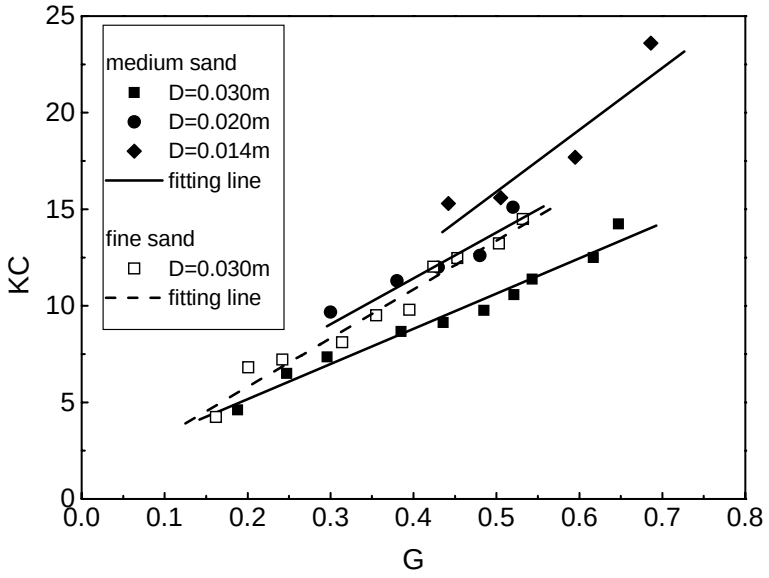


Figure 7: KC and G Correlation (Case I).

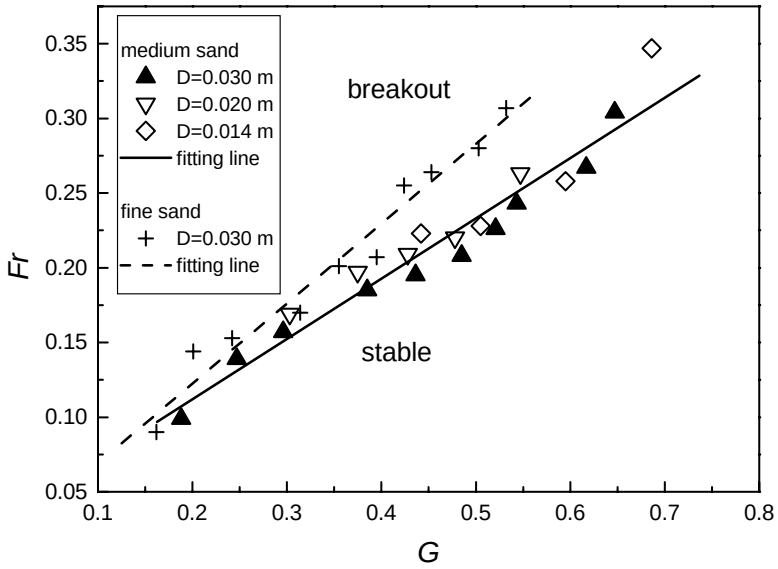


Figure 8: Fr and G Correlation for medium sand (Case I).

Figure 8 shows the correlation between $Fr$ and $G$. For the same sand (medium sand), all the data with different pipe diameters fall within the range with the same linear relationship. There is a good correlation between the Fr number and the G number regardless

of the pipeline diameter. It matches with the point of Chakrabarti (1994) and Poorooshasb (1990), which indicates the importance of $Fr$ in case of water-structure-soil interaction.

However, there exists some deference between the results for medium sand and fine sand, as shown in Figures 7 and 8. That is, the sand characteristics influence pipeline stability.

**Case II: Anti-rolling pipeline**

With the designed anti-rolling device (Figure 3), experiments were conducted on medium sand for pipelines with different diameters, i.e. D=0.030m, 0.020m, as well as different submerged weight. As the experiments on pipelines freely laid, the oscillatory flow amplitude also rises at the same speed $\dot{A}_0$.

Figure 9 shows the correlation between G and KC number for case II. Similar to Case I, for the pipelines with same diameter, KC at which pipelines lose stability increase linearly with G number, but pipeline diameter effect is also very obvious.

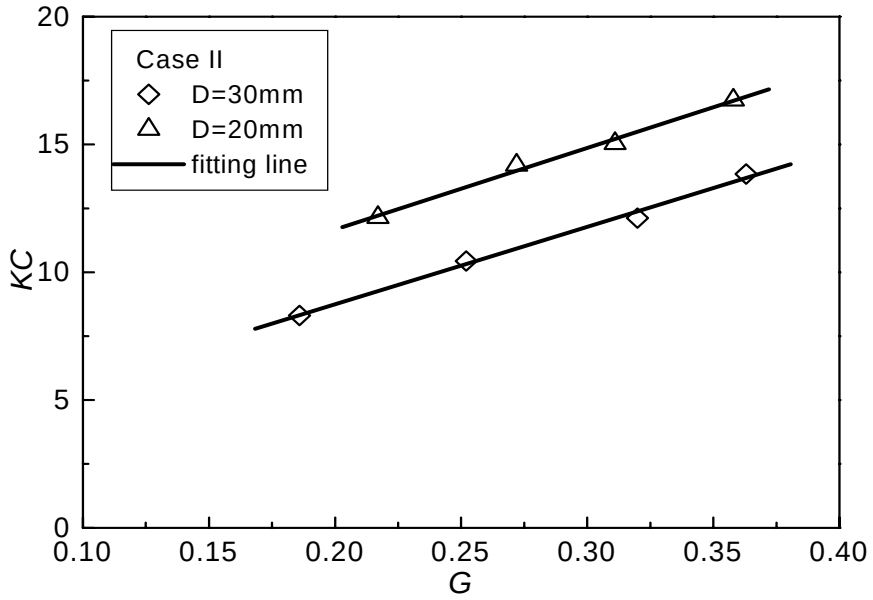


Figure 9: KC and G Correlation (Case II).

Figure 10 shows the correlation between $Fr$ and $G$ for Case II. All the data with different pipe diameters fall within the range with the same linear relationship, as Case I shown in Figure10.

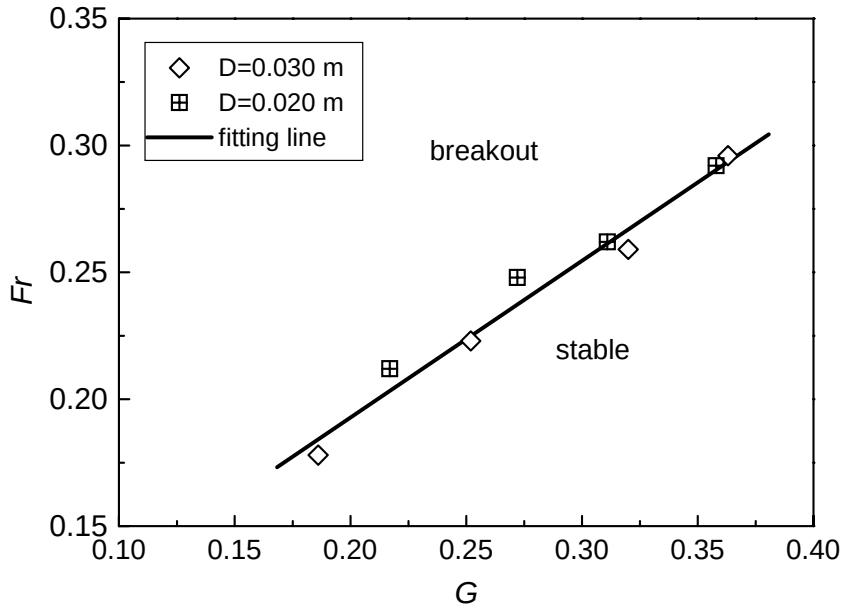


Figure 10: Fr and G Correlation (Case II).

Herein, it should be mentioned that the experiment results are obtained under the condition of the oscillatory flow amplitude rising at the same speed $\dot{A}_0$. As to the pipelines with different submerged weights, the Fr numbers at which pipelines lose stability are different. Thus the oscillating time (*t/T*) is different in different experiments. Their ranges for Case I and Case II are about 80-300, 170-230 respectively. Under the oscillating actions, the effective stress field and pore-pressure field will change with time. When the oscillatory flow velocity exceeds a certain value, the sand beside pipeline is scoured under the influence of vortexes. The sand ripples are formed step by step. They will affect the flow field near pipeline and even influence pipeline instability.

In addition, the Fr-G relationships for the two constrains are obtained within the certain rang of no-dimensional parameter G. As mentioned, $KC$ can be satisfied concurrently with $Fr$ during model tests. The KC range in the experiments is about 5-20.

## 2.5.3. Effects of loading history

In the aforementioned experiments, the same wave loading method was adopted, to examine the instability induced by rapidly increasing storm. However, real storm wave events are unpredictable and the field conditions are often characterized with significant uncertainty.

Thus, it is also very necessary to study the effects of loading history upon the pipeline instability.

### *A. Effects of loading velocity*

Firstly, various loading velocities are employed respectively, i.e. a) $\dot{A}_0 \approx 4.5\times10^{-3} cm/s$; b) $\dot{A}_0 \approx 9.0\times10^{-3} cm/s$, c) $\dot{A}_0 \approx 1.8\times10^{-2} cm/s$ as shown in Figure 11. The test pipe has the diameter of 0.030m, submerged weight of 4.22N/m. The constraint condition is chosen as Case I. The test sand is a kind of medium sand, whose properties are listed in Table 1.

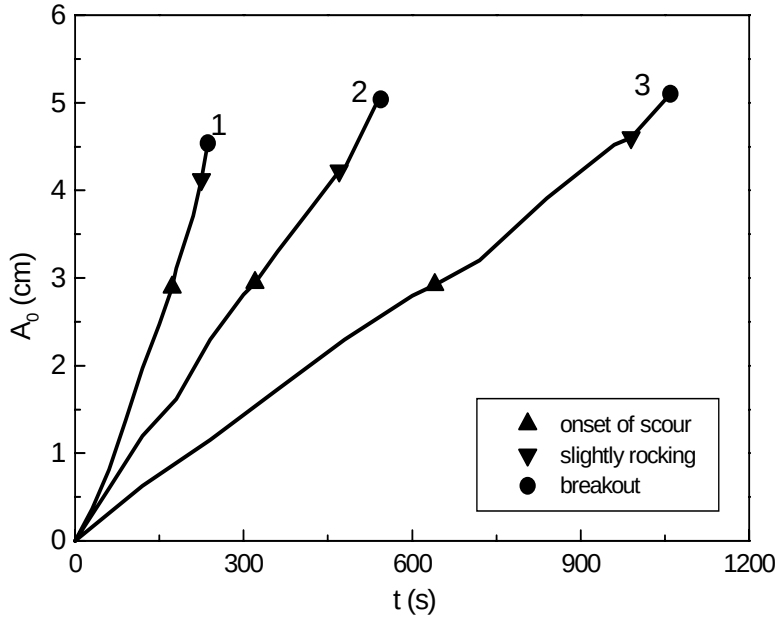


Figure 11: Effects of loading velocity on pipe stability.

Figure 11 shows that with the increase of $\dot{A}_0$, the oscillatory flow amplitude at which the pipe rocks slightly and the amplitude at which pipe loses stability increase respectively, but the amplitude of oscillatory flow induced sand scouring is affected slightly.

Experimental observation indicates, that the smaller of $\dot{A}_0$, the higher sand dune is formed beside pipe, at the time when the pipe is losing stability. As analyzed in Section

2.3, $\dot{A}_0 << U_m$, thus the change of $A_0$ is quasi-static at specific value of $U_m$ (or $A_0$). Various $\dot{A}_0$ represents somehow the different oscillating times (*t/T*) at the vicinity of certain value of $U_m$. Therefore, the loading velocity (or the oscillating times) affects the sand scouring around pipe and eventually has influence on the stability of pipe.

### *B. Effects of long-lasting oscillation at various amplitudes*

The storm growing is not always continuous, at different sea fields or various seasons at same sea field. Sometimes, long-lasting oscillation at various amplitudes occurs. To consider this situation, experiments with the following four types of loading history have been conducted, as shown in Figure 12.

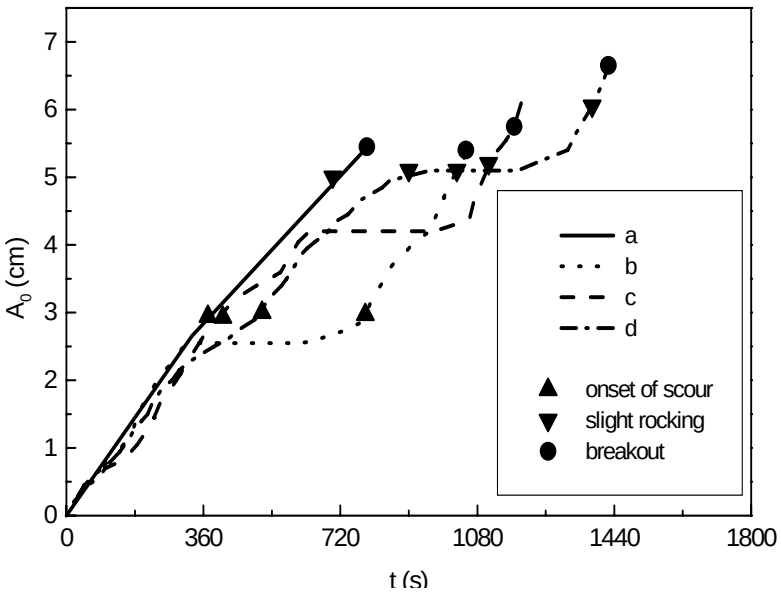


Figure 12: Effects of long-lasting oscillating amplitude on the pipe stability.

*Type a:* The amplitude increases at a constant velocity $\dot{A}_0 \approx 9.0 \times 10^{-3} cm/s$;

*Type b:* The flow amplitude firstly increases at the former velocity till $A_c$ = 2.60 cm, then maintains at $A_c$ for 5 minutes, i.e. about 115 cycles, and finally increases as before.

*Type c:* Similar to Type b, except for $A_c$ =4.15cm.

*Type d:* The flow amplitude firstly increases with the former velocity till $A_c$ at which the pipe rocks slightly, then maintains at $A_c$ 115 cycles, and finally increases as before.

Figure 12 indicates that when long-lasting oscillatory amplitude $A_c$ less than that of onset of scour $A_s$ (Type b), it nearly does not have influence on the pipe stability. When $A_c > A_s$ (Type c, d), due to the effect of vortex, the sand grains pile up on both sides of the pipe, thereby the long-lasting oscillation increases the stability of pipeline. Furthermore, the pipe slight rocking is not always followed by losing stability. If the flow amplitude dose not rise after pipe begins lightly rocking, the pipe will return to the static condition again and the more sediment is observed piling beside the pipe (Type d). After the flow amplitude increases to some higher level, the pipe slightly rocks again, and loses stability at higher flow amplitude.

All above imply that the wave-induced pipe instability is coupled with the sand scouring around pipe, and some intermittently growing storm could be beneficial for the pipe stability.

## 2.6 Comparison with previous experiments

The above experimental results show that, under the action of rapidly rising wave induced wave loading, there exist different linear relationships between Fr and G numbers for freely laid pipelines and anti-rolling pipelines respectively. As to the medium sands, the least square fitting equations of the data in Figures 8 and 10, can be given as

$$\frac{U_m}{\sqrt{gD}} = \begin{cases} 0.043 + 0.37\dfrac{W_s}{\gamma' D^2} \quad (0.18 < \dfrac{W_s}{\gamma' D^2} < 0.65) & freely\ laid\ \ pipes \\ 0.069 + 0.62\dfrac{W_s}{\gamma' D^2} \quad (0.18 < \dfrac{W_s}{\gamma' D^2} < 0.36) & anti-rolling\ \ pipes \end{cases} \tag{20}$$

The equations give the relationships between water particle velocity, soil properties, pipe diameter and submerged weight of the pipe. All the parameters involved have obvious physical meaning. This line can be regarded as the critical line for pipe on-bottom instability. However, in the previous experiments (Allen, 1989; Brennodden et al., 1986; Wagner et al., 1987; Brennodden et al., 1989), mechanical actuator was used to simulate the real hydrodynamic forces upon pipelines. So the pipe-soil interaction models obtained by the experiments do not include wave parameters (see Eqs. (1), (2) and (3)). In order to compare

with the previous experiment results, the calculation of hydrodynamic forces induced by waves on pipeline is essential.

### 2.6.1 Calculation of the wave-induced forces upon pipeline with Wake II model

Historically, the wave-induced forces upon submarine pipeline used to be calculated with an adaptation of Morison's equation for both horizontal and vertical or a lift force taken to be proportional to the ambient velocity squared. However, it has been recognized that in the force model, the ambient velocity should be modified under the consideration of wake flow. Measurements showed that Morison's equation is lacking in its ability to predict the details in shape and magnitude of force time history.

Soedigdo et al. (1999) proposed a Wake II model, in which wake velocity correction was derived based on a closed-form solution to the linearised Navier-Stokes Model for oscillatory flow and hydrodynamic forces coefficients were determined based on start-up effects. Wake II model can be used for stability design calculations for pipelines on the seabed for regular waves without currents for various diameters. Sabag et al. (2000) pointed out that the Wake II model fitting well with experiment results, and it is a great improvement on Morison's equation. The Wake II model is summarised in Appendix.

Take the experiment on anti-rolling pipe with $W_s$ =2.04 N/m, D=0.030 m as an example (see Figures 13 and 14). Figure 13 shows the difference between the amplitude of $U_e$ and that of $U(t)$ gets bigger with the increase of free stream velocity. The correction for wake velocity can significantly increase the effective velocity encountered by pipeline. The free stream, effective and wake velocities calculated with Wake II model are conceptually illustrated in Figure 14. With. (24) to (27), the lift force and horizontal force can be calculated, as shown in Fig. 15.

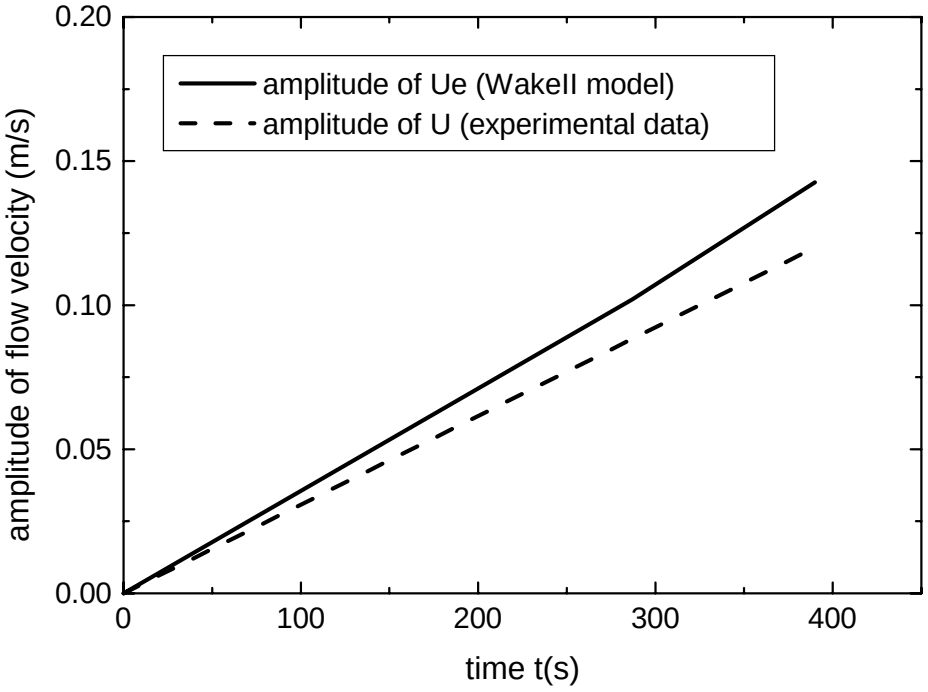


Figure 13: The increasing of oscillatory flow amplitude (D=0.030m).

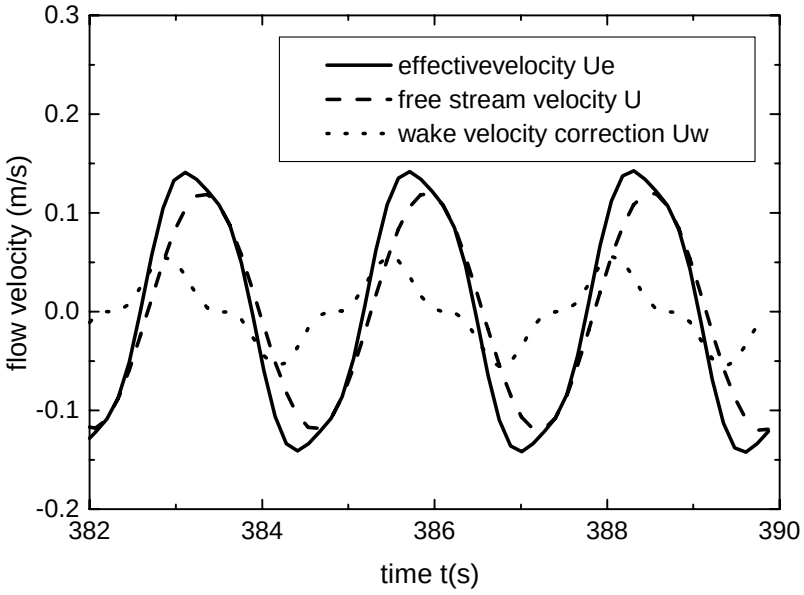


Figure 14: The effective, free stream and wake velocities (D=0.030m).

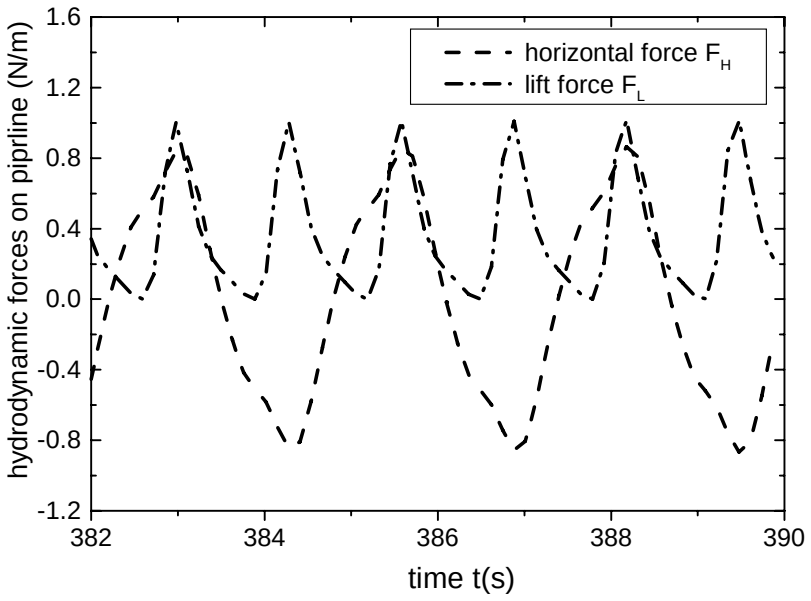


Figure 15: Lift and horizontal forces on pipeline with Wake II (D=0.030m).

Figure 16 shows lift forces calculated with Wake II model and those predicted for the lift forces using Morison's equation. The predicted lift forces from Morison's equation are much smaller than that from Wake II model, since it reflects only the ambient velocity magnitude. Typical horizontal force comparisons are shown in Figure 17. The predicted horizontal forces from the Morison's equation are in close agreement with the horizontal forces predicted with Wake II model.

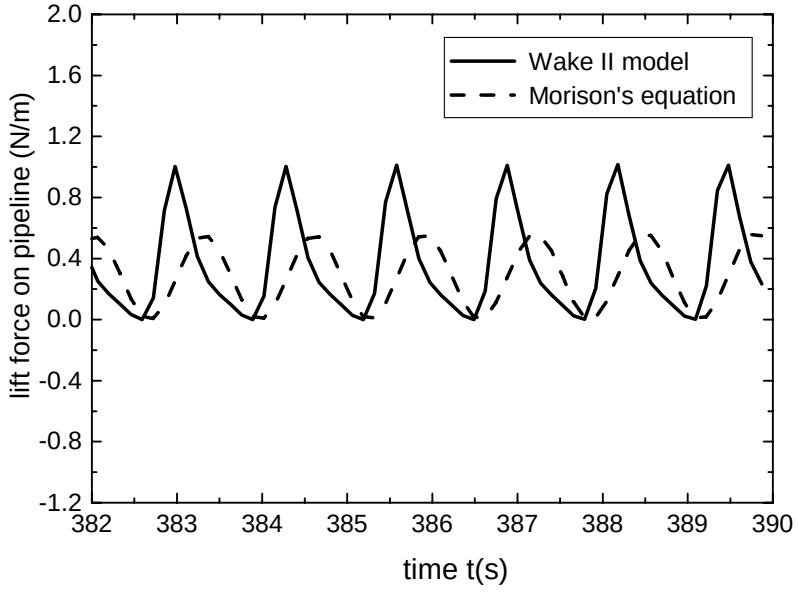


Figure 16: Lift forces with Morison's equation and Wake II model (D=0.030m).

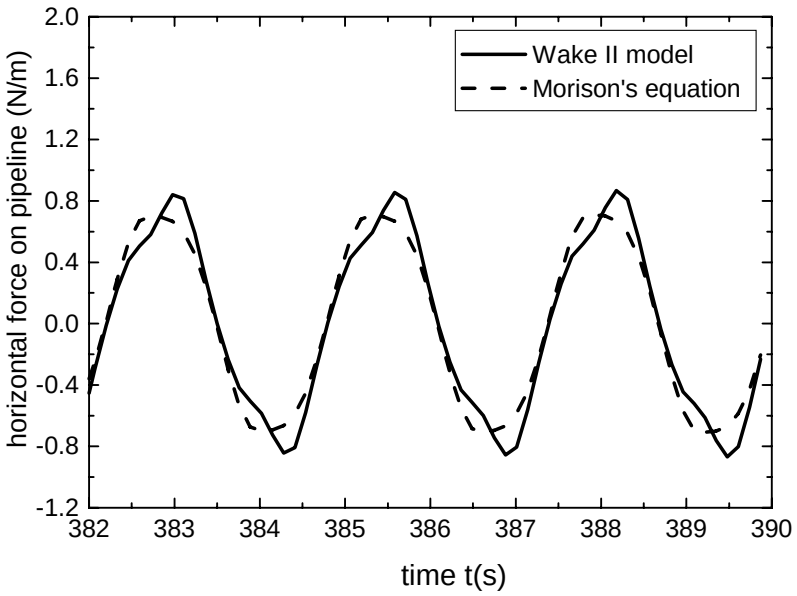


Figure 17: Horizontal forces with Morison's equation and Wake II model (D=0.030m).

## 2.6.2. Comparison with 'pipe-soil' interaction experiments

As discussed in section 2.6.1, under the rapidly increasing wave loading, the pipe suddenly moves away from its original site after a period of slight moving. During the breakout process, the pipeline must conquer the maximum soil resistance. The maximum coefficient $\mu$ of soil resistance can be expressed as

$$\mu = \left( \frac{F_H(t)}{W_s - F_L(t)} \right)_{\max}, \tag{21}$$

where $F_H(t)$ and $F_L(t)$ are calculated with (25) and (27) respectively. Thus, given the ambient velocities during the full period of pipe's losing stability, the maximum value of soil resistance can be obtained.

The maximum values of soil resistance for anti-rolling pipelines on medium sand are shown in Figure 18, together with that in previous 'pipe-soil' interaction experiment results of Wagner et al (1987). Typical test results of Brenodden et al (1986) are given in Figure 19. The average value of soil resistance in our experiments is about 0.83, which is larger than the value obtained in previous pipe-soil interaction experiments. In the present experiments, the medium sand is moderate dense, whose relative density is 0.37. Therefore, though our

experiments are conducted with different loading style from previous pipe-soil interaction experiments, their results are comparable with the later and more reasonable in the mechanism aspects for reflecting the coupling of wave-pipe-soil. Because of the insufficiency of the test data, the final model has not been obtained yet, but the relationships imply that they can serve as a supplementary analysis tool for pipeline stability.

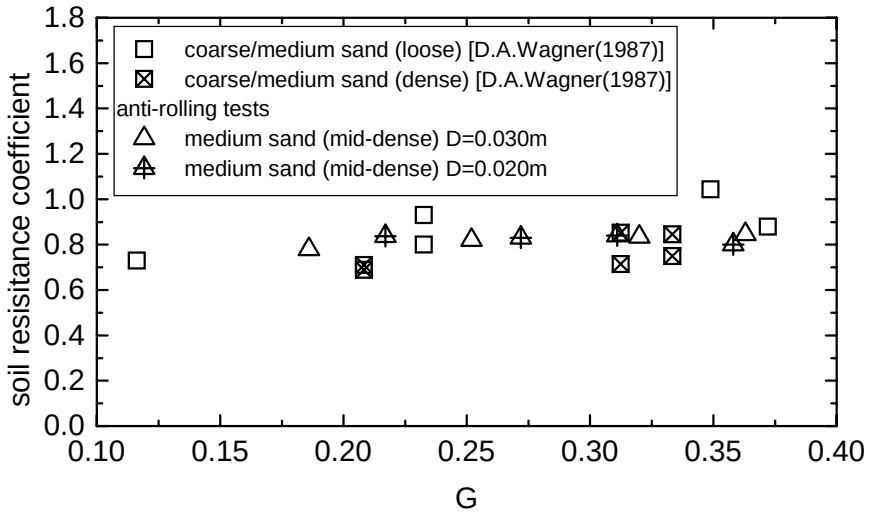


Figure 18: Comparison with 'pipe-soil' interaction experiment results of Wagner et al (1987).

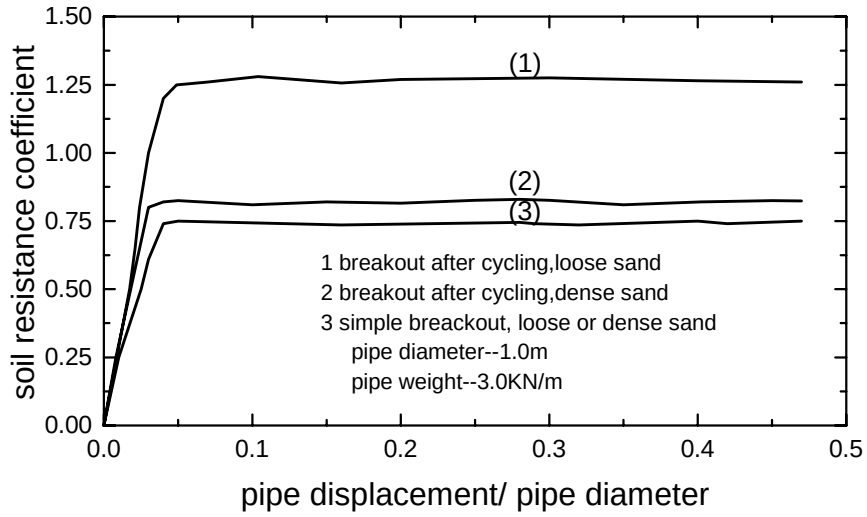


Figure 19: Typical test results of Brenodden et al (1986).

# 3. New Design Method[1]

## 3.1 Existing design models

During recent decades, offshore pipelines have become one of efficient practices of transport for oil and gas. When pipelines are installed upon seabed and subjected to wave loading, there exits a complex interaction between waves, pipelines and seabed. To avoid the occurrence of lateral instability of a pipeline, the pipeline has to be given a heavy weight of concrete coating or alternatively be anchored/trenched. Both methodologies are expensive and complicated from the aspects of design and construction. The weight of concrete coating is a decisive factor for the accomplishment of satisfactory pipeline stability and it may prove to be the decisive factor for carrying out the installation. In the current pipeline engineering practice, however, mistakes or inconsistence often occurs in the design of pipeline (Lawlor and Flynn 1991). The importance of a safe and economic design of submarine pipeline with respect to its on-bottom stability has been widely recognized, which urges the need for a more reliable design method.

The state-of-the-art in pipeline stability design has been changing very rapidly recently. A few investigations have addressed the problem of pipeline-seabed interaction, such as PIPESTAB project (Brennodden *et al*. 1986; Wagner *et al*. 1987), the AGA project (Brennodden *et al*. 1989) and a project at Danish Hydraulic Institute (DHI) (Palmer et al. 1988). The PIPESTAB and AGA projects have produced soil resistance models, e.g. the Pipe-Soil Interaction Model (Wagner *et al*. 1987) and the Energy-Based Pipe-Soil Interaction Model (Brennodden *et al*. 1989). In the previous models, which were drawn from mechanical actuator loading experiments, the complicated behavior of submarine pipelines subjected to ocean environmental loads was reflected to a certain extent. These include the pipeline embedment, which occurs as a pipeline is laid upon the seabed, and the additional settlement during oscillatory loading history. In the Pipe-Soil Interaction Model, the total soil lateral resistance to pipeline movement, $F_H$, was assumed as the sum of sliding resistance component and soil passive resistance component, i.e.

$$F_H = \mu(W_s - F_L) + \beta\gamma' A_T \tag{22}$$

[1] Part of this section forms the manuscript: Gao, F. P., Jeng, D-S; and Wu, Y.: An improved analysis method for wave-induced pipeline stability on a sandy seabed. Journal of Transportation Engineering, ASCE (submitted)

where $\mu$ is the sliding resistance coefficient, $W_s$ is the pipeline submerged weight per meter, $F_L$ is the wave induced lift force upon pipeline, $\beta$ is an empirical coefficient, $\gamma'$ is the soil buoyant weight, $A_T$ is the half value of the contact area between pipeline and soil. From (1), the submerged weight of pipeline ($W_s$) for maintaining pipeline stability can be calculated by

$$W_s = (F_H - \beta\gamma' A_T + \mu F_L) / \mu \tag{23}$$

The above Pipe-Soil Interaction Model has been adopted in the existing DnV Recommended Practice (Det norske Veritas 1988). The lateral soil resistance ($F_H$) should balance the designed wave loads upon pipeline, which can be calculated with the Wake Model proposed by Lambrakos *et al*. (1987), which takes into account of the effect of the wake generated by oscillatory flow over pipeline. In the existing DnV Practice, three different methods are included, namely Dynamic Analysis Method, Generalized Stability Analysis Method and Simplified Stability Analysis Method (Det norske Veritas 1988). Herein, we outline these three methods:

- The Dynamic Analysis Method involves a full dynamic simulation of a pipeline resting on the seabed, including modeling of soil resistance, hydrodynamic forces, boundary conditions and pipe dynamic response. Dynamic analysis forms the reference base for the Generalized Analysis Method. It may only be used for detail analysis of critical areas along pipeline, such as pipeline crossings, riser connections etc., where the details of pipeline response are required, or for reanalysis of a critical existing pipeline.

- The Generalized Stability Analysis is based on a set of non-dimensional stability curves, which have been derived from a series of runs with a dynamic response model. This method may be used for the design of the pipeline sections where potential pipeline movement may be important. The Generalized Analysis Method includes a complete-stable-pipeline design criterion for the special sections of a pipeline.

- The Simplified Stability Analysis Method is for the design of common sections of a pipeline, to which an accumulative lateral displacement is allowable. It is based on a quasi-static balance of forces acting on the pipe, but has been calibrated from the Generalized Stability Analysis. The method generally gives pipe weights that form a conservative envelope of those obtained from the Generalized Stability Analysis.

It is noted that, in the DnV Practice, the evaluation of soil resistance to pipeline movement and that of wave loads upon pipeline are conducted separately. The Pipe-Soil

Interaction Model was found to be conservative for determining the weight coating of pipeline (Verley and Reeds 1989). As stated by Lawlor and Flynn (1991) and Hale *et al*. (1991), the underlying physical mechanism of pipeline on-bottom stability has not yet been well understood.

In the previous experiments (Brennodden *et al*. 1986, Wagner *et al*. 1987, Brennodden *et al*. 1989 and Palmer *et al*. 1988), the wave-induced hydrodynamic forces upon pipeline were simulated with a mechanical actuator. In their experiments, the test pipeline was attached to the mechanical rig by a suspension system, which provided the transfer of the horizontal and vertical forces simulating the wave loads on pipeline. In the models proposed by Wagner *et al*. (1987) and Brennodden *et al*. (1989) etc., numerous empirical coefficients have no implicit physical meanings and are difficult to determine in design procedure. In reality, the wave forces act on not only pipeline but also seabed, and the seabed response to the hydrodynamic forces can affect the pipeline stability too. Therefore, precisely speaking, the wave induced on-bottom stability of the submarine pipeline involves the interaction of wave, soil and pipe, but not pipe/soil interaction.

Unlike the aforementioned experimental methods, Gao *et al*. (2002; 2003) have studied intensively the pipeline on-bottom stability with a U-shaped oscillatory flow tunnel, as shown in Figures 1 and 2. The U-shaped oscillatory flow tunnel is made of transparent plexiglass with section area of $0.2 \times 0.2$ m$^2$. By a butterfly-valve periodically opening and closing at the top of a limb of the water tunnel, the water was capable of accomplishing a simple harmonic oscillation for simulating the wave induced oscillating movement of water particles near the seabed. By regulating valve, the effective air flux from air blower can be changed. Thus, the amplitude can be varied continuously from 5 to 200 mm. The lower part of the water tunnel constitutes the test section with a soil box filled with sand regarded as sandy seabed. The test pipe was directly laid upon the surface of sand, as shown in Figures 1 and 2.

It has been well known that even small change in the thickness of concrete coating may pose significant impact on the entire pipeline project (Allen et al. 1989). As such, a more reasonable analysis method for pipeline on-bottom stability is highly desired.

The objective of the paper is to propose an improved analysis method for pipeline on-bottom stability from the aspect of wave-pipe-soil interaction. A comparison will be made between the physical phenomena of pipe losing stability in the pipe-soil interaction tests and those in the wave-pipe-soil interaction tests. Based on the relationships for describing pipeline on-bottom stability induced by waves, the analysis procedure will also be presented.

Furthermore, the submerged weights of pipeline predicted by the improved analysis method will be compared with those by DnV Practice (Det norske Veritas 1988).

## 3.2 Physical Phenomena of Pipeline Losing On-Bottom Instability

In the PIPESTAB, AGA and DHI pipe-soil interaction tests, the instability process of pipeline was either displacement controlled or force controlled. In their experiments, when losing lateral stability, pipe was pushing the soils nearby back and forth and sand scouring was not involved (Allen *et al*. 1989). Both the PIPESTAB and AGA pipe-soil interaction tests have generally showed that any loading history causing additional pipeline penetration would result in an increase of lateral resistance. These results can be explained by the importance of pipe penetration into the soil, mounding in front of the pipe and the associated lateral earth passive pressure. With the increase of the sand density, the effect of cyclic preloading on the ultimate soil resistance became less, due to the reduced initial penetration in the dense sand and reduced penetration increase with cyclic loading on the dense sand compared with those for loose sand (Wagner *et a*l. 1989). However, in oscillatory flow conditions, the traditional static stability of pipe-soil interaction is not necessarily valid. This is particularly true in the weak bottom soils typical of the upper layer of some marine sediments (Lammert and Hale 1989).

In the wave-pipe-soil interaction experiments with U-shaped oscillatory tunnel (see Figure 1), a constant value of the increase of oscillatory flow amplitude per second, i.e. $\dot{A}_0 = 0.09 \times 10^{-3}$ m/s, was adopted for exploration of the mechanism of pipeline instability induced by rapidly increasing storm waves. With the increase of oscillatory flow amplitude, three characteristic times are experienced during pipe losing on-bottom stability (see Figure 5): (a) Onset of scour: local scour is triggered when water particle velocity around pipe is large enough, thereafter sand ripples will be gradually formed in the vicinity of the pipe; (b) Pipe rocking: the pipe rocks slightly periodically at its original location with approximately same frequency of oscillatory flow; (c) Pipe breakout: the pipe suddenly moves away from its original location, or breakout takes place, after a period of slight rocking. The above process of pipeline's losing on-bottom stability has been further verified in the wave flume tests by Teh et al. (2003).

A comparison between the physical phenomena of pipe losing stability in the pipe-soil interaction tests and those in the wave-pipe-soil interaction tests shows that, an additional

penetration of pipe into soil bed under cyclical pre-loadings has been found in both experiments, which increases the ultimate lateral resistance. In the wave-pipe-soil interaction tests, sand scour around test pipe was detected and the sediment transportation was found to have influence on pipe on-bottom stability. However, this could not be simulated in the previous pipe-soil interaction tests. The local sour around marine structures has been recently summarized by Sumer *et al*. (2001) and Sumer and Fredsøe (2002).

## 3.3 New Criteria for Pipeline On-Bottom Instability

Dimensional analysis has indicated that the critical pipeline submerged weight ($W_s/\gamma' D^2$) to keep pipeline laterally stable is mainly relative to the following parameters:

$$W_s/\gamma' D^2 = f(U_m/(gD)^{0.5},\ U_m T/D,$$

$$U_m D/\nu,\ t/T,\ \dot{A}_0/U_m,\ \rho_{sat}/\rho_w,\ D/d_s,\ D_r,\ \kappa,\ldots\ldots) \quad (24)$$

where $W_s$ is the pipeline submerged weight per meter, $\gamma' = (\rho_{sat} - \rho_w)g$ is the buoyant unit weight of soil, $D$ is the outer diameter of pipeline; $U_m/(gD)^{0.5}$ is the Froude number (*Fr*), whose physical meaning is the ratio of inertia force to gravitational force; $U_m$ is the maximum value of the velocity of water particles at seabed, $g$ is the gravitational acceleration; $U_m T/D$ is the Keulegan-Carpenter number ($KC$), which controls the generation and development of vortex around pipeline; $T$ is the wave period; $U_m D/\nu$ is the Reynolds number (*Re*), whose physical meaning is the ratio of inertia force to viscous force; $\nu$ is the kinematic viscosity of fluid ; $t/T$ is the time of oscillatory flow acting on pipeline, $t$ is the loading time; $\dot{A}_0/U_m$ is the ratio of the increase of oscillatory flow amplitude per second ($\dot{A}_0$) to the maximum of water particle velocity; $\rho_{sat}/\rho_w$ is specific gravity of saturated sand, i.e. the ratio of the density of saturated sand ($\rho_{sat}$) to that of pore water ($\rho_w$); $D/d_s$ is the ratio of pipe diameter ($D$) to particle diameter of sand ($d_s$); $D_r$ is the relative density of sand; $\kappa$ is the relative roughness of pipeline (Gao *et al*. 2003).

Since both *Fr* and Re could not be satisfied concurrently in the wave experiments, it is reasonable to employ the *Froude* scaling process and allowance were made for variation in *Reynolds* number (Chakrabarti 1994). In the experiments, Re range is at the order of $10^3 - 10^4$, which is approximately one order less than that in the field. Based on the experimental

results, the criteria for the stability of smooth pipelines ( $\kappa \approx 0$ ), on a medium-dense sand (*Dr* = 0.37) for two kinds of constraints, i.e. the pipe is free at its ends (Case I) and the pipe is constrained against rolling (Case II), have been established, respectively (see Figure 20)

$$U_m/(gD)^{0.5} = 0.042 + 0.38 W_s/(\gamma' D^2) \qquad for\ Case\ I, \tag{25}$$

$$U_m/(gD)^{0.5} = 0.069 + 0.62 W_s/(\gamma' D^2) \qquad for\ Case\ II. \tag{26}$$

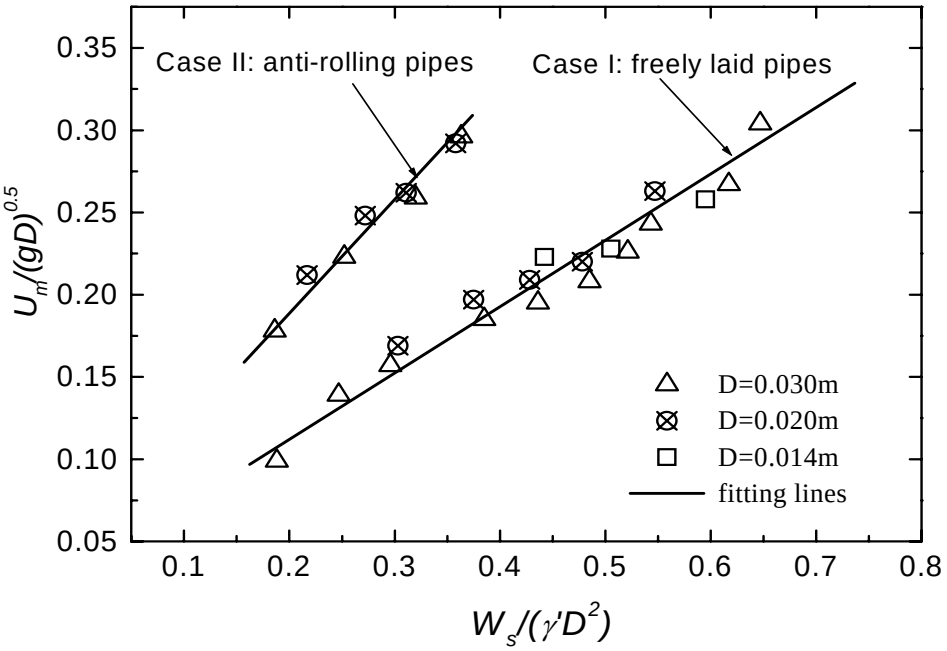


Figure 20: $U_m/(gD)^{0.5}$ and $W_s/(\gamma' D^2)$ correlation for pipeline on-bottom stability (medium sand: *Dr*=0.37, $\gamma'$=9.0 $kN/m^3$)

The above empirical relationships are based on dimensional analysis and fitted to laboratory data. In the equations for describing pipeline on-bottom stability, the parameters for wave, pipe and sand are coupled. The improved empirical model captures the main influential factors for on-bottom stability of pipeline laid upon sandy seabed and provides a better insight into the physical mechanics of pipeline on-bottom instability.

Scale effects should be examined when the results of small-scale wave-pipe-soil interaction tests are extrapolated to real-life situation, where the commonly used pipe diameter is about 0.3 to 1.0 m. The scale effects were investigated initially by running three scales of test pipe diameter, i.e. *D* = 0.014m, 0.020m and 0.030m, respectively (see Figure 20). The figure indicates the scale effects are not obvious when using *Froude* number for data

reduction. However, more large-scale experiments and field observations are desired to further verify the above empirical relationships. It is noted that in the experiments, *KC* range is about 5 to 20, and *Fr* range about 0.1 to 0.3. The seabed properties and loading history would also have influence on the pipeline stability. Thus for various conditions of waves and seabed, some modification should be given to the above wave-pipe-soil interaction relationships for pipeline on-bottom stability.

According the DnV Practice (Det norske Veritas 1988), for a long-distance laid pipeline, the demands for on-bottom stability are different for various sections of the pipeline. Generally speaking, no lateral displacement during extreme environmental conditions is allowed at the special locations, including the section close to a platform, normally taken as 500 m, and some points on pipeline such as valve connections, pipeline crossing, Y- or T-connections expansion loops etc. Certain lateral displacement is acceptable at the common locations, i.e. the section located more than a certain distance away from the platform, normally taken as 500 m. As for the special sections of pipeline, it should keep stable even without the constraint effect from the ends. However, as for the common sections of pipeline, the demands for their stability are less rigorous, i.e. the constraint effect from the ends can be taken into account for their lateral stability. Thus, the obtained relationships in Figure 3 may serve as the criteria for on-bottom stability of pipeline on sandy seabed. The critical line for Case I can be used for evaluating the on-bottom stability of pipeline at special locations, and the one for Case II can be used for evaluating the on-bottom stability of pipeline at common locations, as shown in Figure 21. The critical lines in the figure are based on the medium sand test results, thus they should be modified when the physical parameters of seabed are changed. The new criteria for pipeline on-bottom stability is characterized by

- flat seabed with homogeneous sandy soil conditions along the entire length of the pipeline;
- waves propagating perpendicularly to the pipeline axis;
- materials of pipeline assumed to be rigid compared with soils.

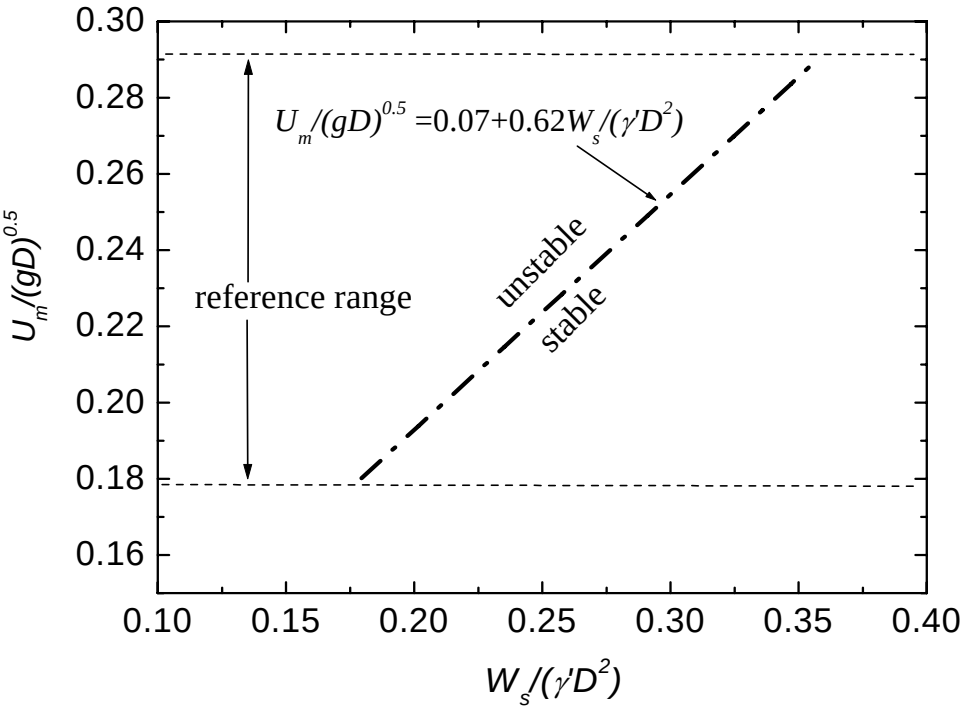


(a)

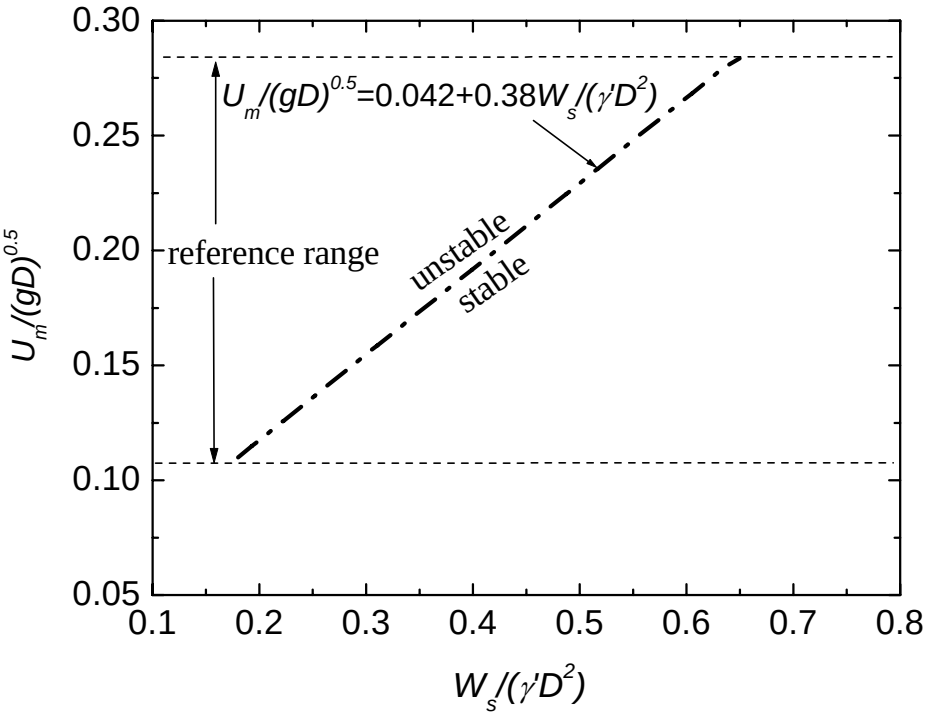


(b)

Figure 21: Criteria for pipeline on-bottom stability on sandy medium seabed: (a) Common sections of pipeline; (b) Special sections of pipeline

## 3.4 Procedure for Analysis of Wave-Induced Pipeline On-Bottom Stability

The aim of pipeline design with respect to the on-bottom stability is to determine the steel pipeline thickness and the weight of the concrete coating or the thickness of concrete coating, so that the submerged weight of the pipeline is sufficient to meet the required stability criteria.

A typical sketch of submarine pipeline wall is illustrated in Figure 22, in which $D_i$ is the inner diameter of pipeline; $t_{st}$, $t_{ac}$ and $t_c$ are the thickness of steel pipeline, antiseptic coating and concrete coating, respectively; $\rho_{st}$, $\rho_{ac}$, $\rho_i$, $\rho_c$ and $\rho_w$ are the mass density of steel, antiseptic coating, transported materials (e.g. oil), concrete coating and water. In engineering design practice, $D_i$, $t_{st}$, $t_{ac}$, $\rho_{st}$, $\rho_{ac}$, $\rho_i$, $\rho_c$ and $\rho_w$ are normally given firstly. The decisive parameter for pipeline on-bottom stability is the thickness of concrete coating ($t_c$).

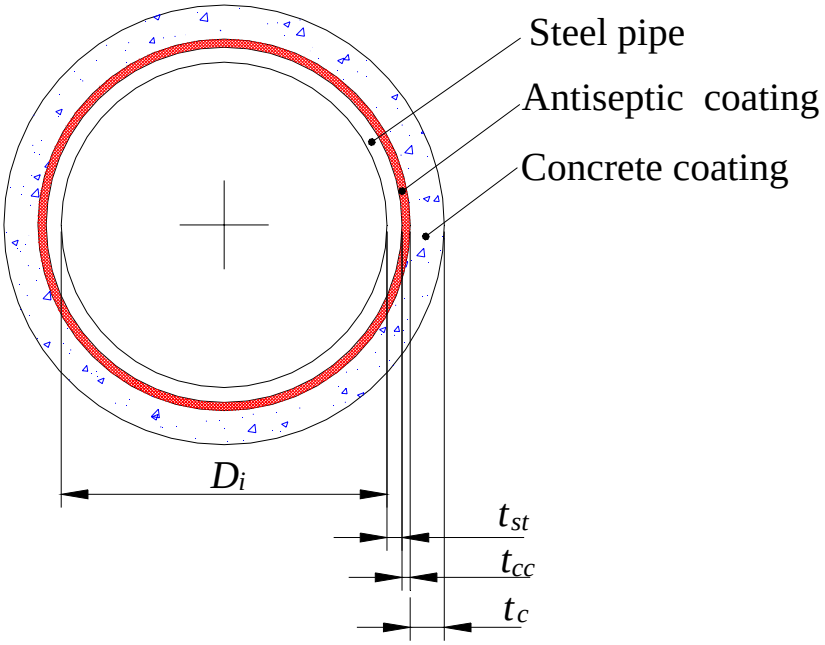


Figure 22: Sketch of submarine pipeline wall

Based on the criteria for pipeline on-bottom stability given in the former section, an improved analysis procedure is suggested, as depicted in Figure 23. In the steps shown in Figure 24, for specific values of wave height (*H*), wave period (*T*) and water depth (*d*), the maximum values of wave-induced particle velocity near seabed bottom ($U_m$) can be obtained based on appropriate wave theories, the range of suitability for which is depicted in Figure 8 (Le Mehaute, 1976). When the values of $d/T^2$ and $H/T^2$ are given, the wave theory can be chosen according to the range of suitability for wave theories as suggested by Le Mehaute (1976). In Stokes' second-order wave theory, the expression for the maximum particle velocity $U_m$ induced by waves is

$$U_m = \frac{\pi H}{T}\frac{ch[k(z+d)]}{sh(kd)} + \frac{3}{4}\left(\frac{\pi H}{T}\right)\left(\frac{\pi H}{L}\right)\frac{ch[2k(z+d)]}{sh^4(kd)}, \qquad (27)$$

in which $k$ is the wave number ($k = 2\pi/L$), $L$ is the wave length, $d$ is the water depth (Sarpkaya and Isaacson 1981). For an untrenched pipeline, the value of $U_m$ is often chosen as that at the middle of pipeline, i.e. $z$=-$d$+0.5$D$. Once the trial value of pipeline outer diameter ($D'$) is given, the Froude number, $U_m/(gD)^{0.5}$, can be calculated, in which $D$ will be replaced with $D'$. Based on the criteria for pipeline on-bottom stability as shown in Figure 4, the corresponding values of the dimensionless pipe weight ($W_s/\gamma' D^2$) can be obtained for the common sections or the special sections of pipeline. The submerged weight of pipeline per meter ($W_s$) can thereby be calculated. Then the calculated value of pipeline diameter ($D$) can be obtained by the following formula,

$$D^2 = \frac{1}{\rho_c - \rho_w}\left[\frac{4W_s}{\pi g} + D_i^2(\rho_{st} - \rho_i) + D_{st}^2(\rho_{ac} - \rho_{st}) + D_{ac}^2(\rho_c - \rho_{ac})\right], \qquad (28)$$

in which $D_{st}$ is the outer diameter of steel pipe ($D_{st} = D_i + 2t_{st}$); $D_{ac}$ is the outer diameter of antiseptic coating ($D_{ac} = D_{st} + 2t_{ac}$). If $\left|D - D'\right|/D$ is larger than the permitting value (e.g. 0.1%), the trail value of pipeline outer diameter $D'$ will be revised. The thickness of concrete coating $t_c$ can be calculated by

$$t_c = (D' - D_i - 2t_{st} - 2t_{cc})/2 \qquad (29)$$

The design value of thickness of concrete coating ($t_{cD}$) is given as

$$t_{cD} = f_t \times t_c \tag{30}$$

Where $f_t$ is the safety factor, normally taken as 1.1 (Det norske Veritas 1988).

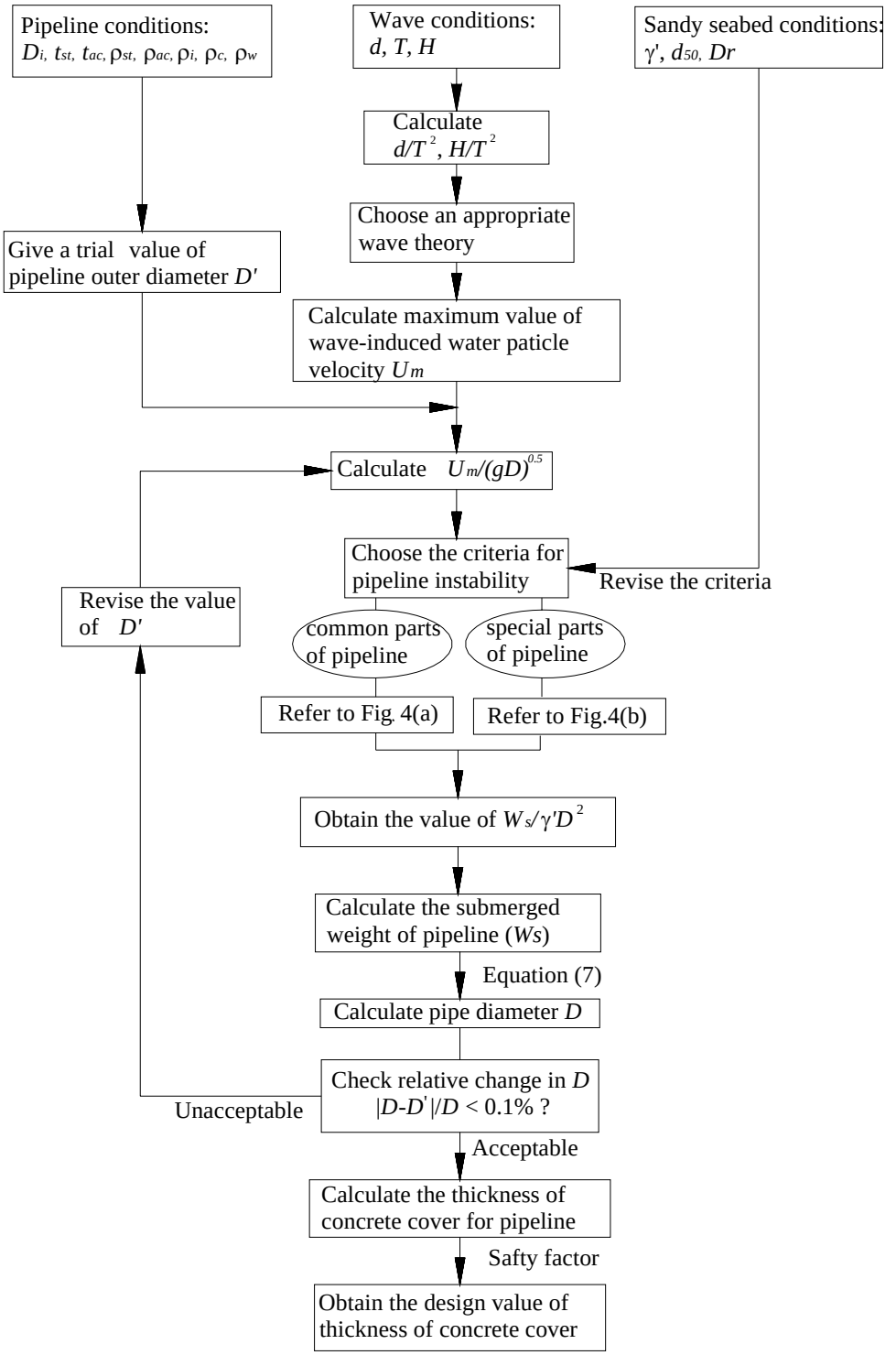


Figure 23: Analysis procedure for pipeline on-bottom stability induced by waves

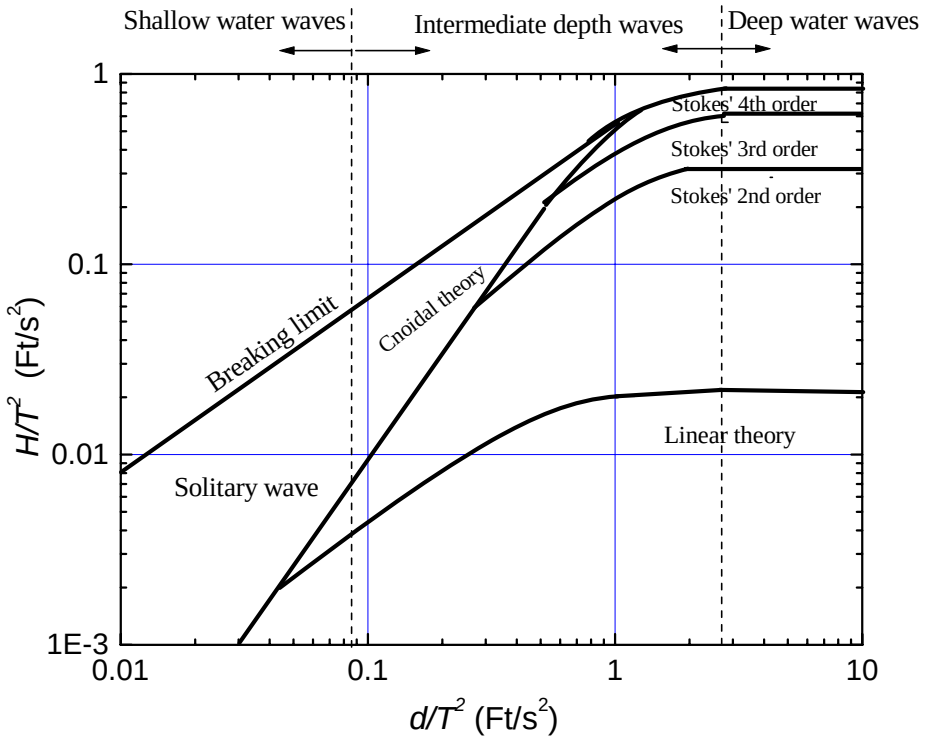


Figure 24: Ranges of suitability for various wave theories (Le Mehaute, 1976)

## 3.5 Comparison with DnV Recommended Practice

The purpose of on-bottom stability design is to determine submerged weight to keep pipe stable at given environmental parameters. To compare the design results of the pipe-soil interaction model with those of the wave-pipe-soil interaction model, a pipeline with inner diameter $D$=0.36 m (approximately 15 inches) is set as an example. The design parameters for pipeline, seabed and waves are listed in Table 3. The properties of sand are chosen the same as those of test sand in wave-pipe-soil interaction experiments; the design wave heights are various, as shown in Table 3.

Based on the Generalized Analysis Method and the Simplified Analysis Method in DnV Practice (Det norske Veritas 1988), the design values of submerged weight ($W_s$) of pipelines at various environmental parameters can be obtained respectively, which are listed in Table 4. Once $W_s$ is gotten, the dimensionless submerged weight of pipeline, $W_s/(\gamma' D^2)$, can be calculated. The values of Froude number, $U_m/(gD)^{0.5}$, can also be calculated. The variations of $U_m/(gD)^{0.5}$ with $W_s/(\gamma' D^2)$ from the Generalized Analysis Method, the Simplified Analysis Method and those from the present new analysis approach are shown in Figure 25.

Table 3: Example of design parameters for wave, seabed and pipeline

| | |
|---|---|
| **Wave characteristics** | |
| Wave period ($T$) | 9.0 (s) |
| Water depth ($d$) | 50 (m) |
| Wave length ($L$) | 125 (m) |
| Wave height ($H$) | 1.7-3.8(m) Various |
| **Seabed (sand) Characteristics** | |
| Mean particle diameter ($d_{50}$) | 0.38 (mm) |
| Buoyant unit weight ($\gamma'$) | $0.9\times10^3$ (N/m$^3$) |
| Relative density ($Dr$) | 0.37 |
| **Pipeline Characteristics** | |
| Inner diameter of pipeline ($D_i$) | 0.36 (m) |
| Thickness of steel pipeline wall ($t_{st}$) | 0.01 (m) |
| Thickness of antiseptic coating ($t_{ac}$) | 0.005 (m) |
| Density of steel pipeline wall ($\rho_{st}$) | $.85\times10^3$ (kg/ m$^3$) |
| Density of transported material e.g. crude oil ($\rho_i$) | $0.95\times10^3$ (kg/ m$^3$) |
| Density of sea water ($\rho_w$) | $1.03\times10^3$ (kg/ m$^3$) |
| Density of concrete coating ($\rho_c$) | $2.40\times10^3$ (kg/ m$^3$) |

Table 4: Design Values of Submerged Weight of Pipelines Based on DnV Practice at Various Environmental Parameters Given in the Table 3

| $H$ /(m) | $J_m$/ (m/s) | $W_s$ / (kN/m) | |
|---|---|---|---|
| | | Simplified Analysis Method | Generalized ysis Method |
| 1.7 | 0.25 | 0.115 | 0.288 |
| 2.1 | 0.30 | 0.149 | 0.374 |
| 2.4 | 0.35 | 0.187 | 0.490 |
| 2.8 | 0.40 | 0.229 | 0.616 |
| 3.1 | 0.45 | 0.277 | 0.748 |
| 3.4 | 0.50 | 0.327 | 0.845 |
| 3.8 | 0.55 | 0.385 | 1.004 |

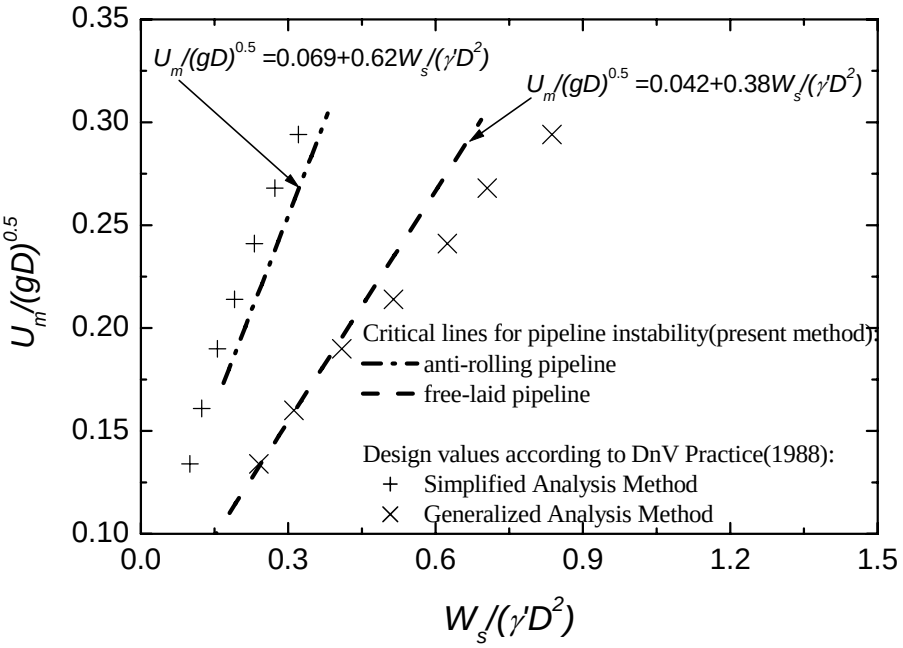


Figure 25: Comparison between the results predicted by DnV Recommended Practice and by present new analysis method

As mentioned preiously, the critical line for freely laid pipelines (Case I) can be used for evaluating the on-bottom stability of pipeline at special sections, and the one for anti-rolling pipelines (Case II) can be used for evaluating the on-bottom stability of pipeline at common sections. It is indicated in Figure 25 that, the critical line for the instability of anti-rolling pipeline and that for free-laid pipeline in the empirical wave-pipe-soil interaction relationships match approximately the design values based on Simplified Analysis Method and those based on Generalized Analysis Method in DnV Practice, respectively. Nevertheless, with the increase of Froude number, the Generalized Analysis Method is getting more conservative for the on-bottom stability design of the pipeline at special sections. This may be explained by that the sand dune that forms in the vicinity of pipeline due to scour, and which benefits pipeline's on-bottom stability. Sand scour, as an indicator of wave-pipe-soil interaction, is one of the influential factors for pipeline stability, which however has not been taken into account in the existing DnV Practice for pipeline stability design.

# 4. Concluding Remarks

(1) Froude number (Fr) and the non-dimensional pipe weight (G) are two most important parameters in modeling wave-induced instability of untrenched pipeline. Based on the experimental results, different linear relationships between Fr and G have been obtained for pipes with different restraint conditions, i.e. a) freely laid pipelines and b) anti-rolling pipelines. Moreover three characteristic times in the process of the pipe's losing stability are revealed.

(2) Based on Wake II model, the current wave-soil-pipe interaction test results and the results of previous pipe-soil interaction tests are compared. It is indicated that the results of two types of tests are comparable. The obtained Fr-G relationships can be used for supplementary analysis of criterion for pipeline instability in design procedure.

(3) In consideration of the actual field conditions, different loading histories are used to explore the effects of them on the pipeline instability. It is found that the scouring of sand besides the pipeline is the main result of the deferent loading histories, and affects the pipeline stability eventually.

(4) Sand scour, as an indicator of the "wave-soil-pipe" coupling, is detected in our experiments. But, in the previous experiments with actuator, it could not be modeled. Therefore, the current hydrodynamic experiments are more reasonable in the mechanism aspects, which reflect the 'wave-soil-pipeline' coupling effects. The physical phenomena of pipeline losing on-bottom stability was better simulated in the wave-pipe-soil interaction experiments, in which local scour around pipeline was detected, reflecting the intensive interaction between wave, pipe and sand. The relationships between $U_m/(gD)^{0.5}$ and $W_s/(\gamma' D^2)$ for two kinds of constraint conditions, i.e. Case I: freely laid pipes, Case II anti-rolling pipes, can serve as the stability criteria for special sections and common sections of the pipeline, respectively.

(5) Based on the obtained relationships between $U_m/(gD)^{0.5}$ and $W_s/(\gamma' D^2)$, an improved analysis method for pipeline on-bottom stability is proposed. The analysis procedure is given with a detailed illustration.

(6) A comparison of submerged weights of pipeline predicted with existing DnV

Recommended Practice and those with the new method indicates that they are generally comparable. With the increase of Froude number, the Generalized Method in the DnV Practice becomes more conservative than the wave-pipe-soil interaction model for the on-bottom stability design of pipeline at special sections. Sand scour has some influence on pipeline stability, which however has not been considered in the existing DnV Practice.

## Acknowledgement

Financial supports by National Natural Science Foundation of China (Project No. 50509022) and 'Tenth Five-year Plan' of Chinese Academy of Sciences (Project No. KJCX2-SW-L03) and Australian Research Council Large Grant Scheme # A00104092 (2001-2003) are greatly appreciated. The second author is grateful for the support from Institute of Mechanics, Chinese Academy of Science under Senior Visiting Scholar Scheme to initialise the second half of this report during December 2004-January 2005. The authors The authors also thank Professors Yingxiang Wu, Xiaoyun Gu, Qun Pu and Senior Engineer Kun Li at Institute of Mechanics, Chinese Academy of Sciences, for their guidance and assistance in the experiments.

# References

Allen DW, Lammert WF, Hale JR and Jacobsen V. (1989). Submarine pipeline on-bottom stability: recent AGA research. The 10th Offshore Technical Conference, paper 6055.

Brennodden, H., Sveggen, O., Wagner, D.A. and Murff, J.D. (1986). Full-scale pipe-soil interaction tests. Proc. Offshore Technology Conference, OTC 5338, 433-440.

Brennodden H, Lieng JT, Sotberg T and Verley RLP. (1989). An energy-based pipe-soil interaction model. The 10th Offshore Technical Conference, paper 6057.

Chakrabarti K. (1994). Offshore Structure Modeling. JBW Printers & Binder Pte. Ltd.

Chiew, Y.M., (1990). Mechanics of local scour around submarine pipelines. Journal of Hydraulic Engineering, ASCE, 116, 515~529.

Det norske Veritas, (1988). On-bottom stability design of submarine pipelines, Recommended Practice E305

Foda MA, Chang J, Law A. (1990). Wave-induced breakout of half-buried marine pipes. Journal of Waterways, Port, Coastal and Ocean Engineering, ASCE., 116:267-286.

Gao, F. P., Gu, X. Y., Jeng, D.-S. and Teo, H. T. (2002) An experimental study for wave-induced instability of pipelines: The breakout of pipelines. Applied Ocean Research, 24(2), 83-90.

Gao, F. P., Gu, X. Y. and Jeng, D. S. (2003). Physical modeling of untrenched submarine pipeline instability. Ocean Engineering, 30 (10): 1283-1304.

Hale, J.R., Lammert, W.F., Allen, D.W., (1991). Pipeline On-bottom stability calculations: Comparison of two state-of-the-art methods and pipe-soil model verification. Proc. 12th Offshore Technology Conference, OTC, paper 6761.

Herbich J.B. (1985). Hydromechanics of submarine pipelines: Design problems. Can.J. Civil Engng, 12, 863~874

Lammert, W. F. and Hale, J. R. (1989). Dynamic response of submarine pipelines exposed to combined wave and current action. Proceeding of Annual Offshore Technology Conference, OTC 6058, 159-170.

Lawlor, CDF, Flynn, SJA. (1991). Subsea pipeline stability analysis: Still a black art? Transactions of the Institution of Engineers, Australia: Civil Engineering, 33: 1-8.

Le Mehaute, B.(1976). An introduction to hydrodynamics and water waves. Dusseldorf: Springer-Verlag.

Lyons, C.G., (1973). Soil resistance to lateral sliding of marine pipelines, Proc. Offshore Technology Conference, OTC, vol. 1876, pp. 479-484.

Mao Y., (1988). Seabed scours under pipelines. Proc 7th Into Symp On Offshore Mechanics and Arctic Engineering (OMAE), ASME, 33-38

Palmer, A. C., Steenfelt, J. S. and Jacobsen, V. (1988). Lateral resistance of marine pipelines on sand, Proceedings of 20th Annual Offshore Technology Conference, Paper OTC 5853, 399-408.

Poorooshasb F. (1990). On centrifuge use for ocean research. Marine Geotechnology, 9:141-158

Sabag, S.R., Edge, B.L., Soedigdo, I.R., (2000). Wake II model for hydrodynamic forces on marine pipelines including waves and currents. Ocean Engineering, 27, 1295-1319.

Sarpkaya, T., and Isaacson, M. (1981). Mechanics of Wave Forces of Offshore Structures. London: Van Nostrand Reinhold Company.

Soedigdo, I.R., Lambrakos, K.F., Edge, B.L. (1999). Predicton of hydrodynamic forces on submarine pipelines using an improved wake II model. Ocean Engineering, 26, 431-462.

Stansby PK, Starr P. (1992). On a horizontal cylinder resting on a sand bed under waves and currents. International Journal for Offshore and Polar Engineering, 2:262-266

Sumer, B.M., Fredsøe, J., (1991). Onset of scour below a pipeline exposed to waves. Int J Offshore and Polar Engng, 1, 189-194

Sumer, B. M. and Fredsøe, J. (2002). The mechanics of scour in the marine environment. New Jersey: World Scientific Publishing Company.

Sumer, B. M., Whitehouse, R. J. S. and Tørum, A. (2001). Scour around coastal structures: a summary of recent research, Coastal Engineering, 44: 153-190.

Teh, T. C., Palmer, A. C., Damgaard, J. S. (2003). Experimental study of marine pipelines on unstable and liquefied seabed. Coastal Engineering, 50: 1 –17.

Verley, R. L. P. and Reed, K. (1989). Response of pipeline on various soils for realistic hydrodynamic loading. Proceedings of 8th Offshore Mechanics and Polar Engineering Conference, 5: 149-156.

Wagner DA, Murff JD, Brennodden H, Sveggen O. (1987). Pipe-soil interaction model. The 8th Offshore Technical Conference, paper 5504.

# Appendix: Wake II Model

Wake II model proposed by Soedigdo et al. (1999), is a hydrodynamic force model for prediction of forces on pipelines. The wake and star-up effects are considered in the model.

The wake velocity correction is corrected by using a closed-form solution to the linearized Navier-Stokes equations for oscillatory flow. By assuming that the eddy viscosity in the wake is only time dependent and of harmonic sinusoidal from, the wake velocity correction affecting pipe in periodic flow can be derived as

$$U_w(t) = \frac{\sqrt{\pi} erf\left(\frac{1}{2} C_2 \sin^n(\omega t + \phi)\right) U_m C_1}{C_2}, \quad \text{(A.1)}$$

where $C_1, C_2, \phi$ and $n$ are empirical parameters relative to current KC number, as shown in Figure A1. The effective velocity $U_e$ can be determined as the summation of the free stream velocity $U(t)$ and the wake velocity correction $U_w(t)$ where as

$$U_e(t) = U(t) + U_w(t) \quad \text{(A.2)}$$

When the effective velocity is known, the force model expression for the drag, lift and inertial forces are:

(a) Drag force:

$$F_D = 0.5\rho_w D C_D(t) |U_e| U_e, \quad \text{(A.3)}$$

(b) Lift force:

$$F_L = 0.5\rho_w D C_L(t) U_e^2, \quad \text{(A.4)}$$

(c) Inertia force:

$$F_I = \frac{\pi D^2}{4} \rho_w \left[ C_M \frac{dU}{dt} - C_{AW} \frac{dU_w}{dt} \right], \quad \text{(A.4)}$$

The horizontal hydraulic force is the sum of drag force and inertia force:

$$F_H = F_D + F_I \quad \text{(A.5)}$$

where, $C_M$ is the inertia coefficient for ambient velocity, $C_M = 2.5$; $C_{AM}$ is the added mass coefficient associated with the wake flow passing the pipe, $C_{AM} = 0.25$; $C_D(t)$ $C_L(t)$ are time dependent drag and lift coefficients and can be determined by so called 'start-up' function, which is relative to the distance the water particle travels after a zero crossing in the total effective velocity.

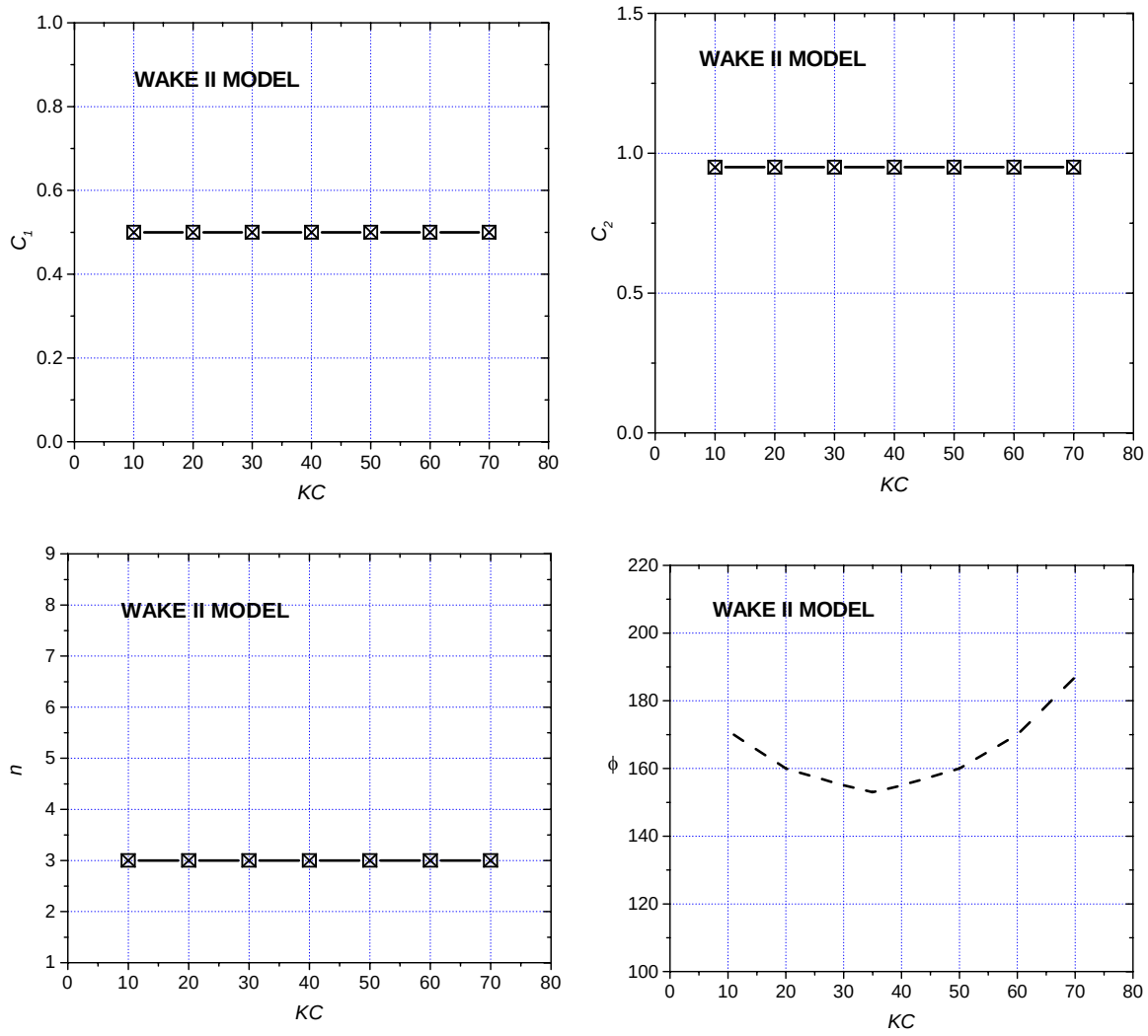


Figure A1: Effect of KC on parameters $C_1, C_2, \phi$ and $n$ (Soedigdo et al., 1999).